technical assistance. This work was supported by grants from the Ministry of Education, Culture, Sports, Science and Technology and the Ministry of Health, Labour and Welfare of Japan.

Authorship contributions

Y. Murakami, R.O., N.I. performed experiments; T.S., H.N., J.N. collected patients' samples; N.I., Y. Maeda and Y.K. discussion; Y. Murakami and T.K. designed the research and wrote the paper.

Competing Interests

The authors have no competing interests.

Supporting Information

Additional Supporting information may be found in the online version of this article:

Fig S1. Distribution of the relative expression of HMGA2 in the patients and the control.

Fig S2. Methylcellulose colony assays of the HMGA2 transduced mouse bone marrow cells.

Fig S3. Distribution of the relative expression of let-7 family in the patients and the control.

Table S1. The summary of PNH patients analyzed in this paper.

Data S1. Materials and methods.

Please note: Wiley-Blackwell are not responsible for the content or functionality of any supporting materials supplied by the authors. Any queries (other than missing material) should be directed to the corresponding author for the article.

References

Ashar, H.R., Fejzo, M.S., Tkachenko, A., Zhou, X., Fletcher, J.A., Weremowicz, S., Morton, C.C. & Chada, K. (1995) Disruption of the architectural factor HMGI-C: DNA-binding AT hook motifs fused in lipomas to distinct transcriptional regulatory domains. *Cell*, **82**, 57–65.

Ayoubi, T.A., Jansen, E., Meulemans, S.M. & Van de Ven, W.J. (1999) Regulation of HMGIC expression: an architectural transcription factor involved in growth control and development. *Oncogene*, **18**, 5076–5087.

Cavazzana-Calvo, M., Payen, E., Negre, O., Wang, G., Hehir, K., Fusil, F., Down, J., Denaro, M., Brady, T., Westerman, K., Cavallesco, R., Gillet-Legrand, B., Caccavelli, L., Sgarra, R., Maouche-Chretien, L., Bernaudin, F., Girot, R., Dorazio, R., Mulder, G.J., Polack, A., Bank, A., Soulier, J., Larghero, J., Kabbara, N., Dalle, B., Gourmel, B., Socie, G., Chretien, S., Cartier, N., Aubourg, P., Fischer, A., Cornetta, K., Galacteros, F., Beuzard, Y., Gluckman, E., Bushman, F., Hacein-Bey-Abina, S. & Leboulch, P. (2010) Transfusion independence and HMGA2 activation after gene therapy of human beta-thalassaemia. *Nature*, **467**, 318–322.

Fedele, M., Visone, R., De Martino, I., Troncone, G., Palmieri, D., Battista, S., Ciarmiello, A., Pallante, P., Arra, C., Melillo, R.M., Helin, K., Croce, C.M. & Fusco, A. (2006) HMGA2 induces pituitary tumorigenesis by enhancing E2F1 activity. *Cancer Cell*, **9**, 459–471.

Hauke, S., Leopold, S., Schlueter, C., Flohr, A.M., Murua Escobar, H., Rogalla, P. & Bullerdiek, J. (2005) Extensive expression studies revealed a complex alternative splicing pattern of the HMGA2 gene. *Biochimica et Biophysica Acta*, **1729**, 24–31.

Ikeda, K., Mason, P.J. & Bessler, M. (2011) 3'UTR-truncated Hmga2 cDNA causes MPN-like hematopoiesis by conferring a clonal growth advantage at the level of HSC in mice. *Blood*, **117**, 5860–5869.

Inoue, N., Izui-Sarumaru, T., Murakami, Y., Endo, Y., Nishimura, J., Kurokawa, K., Kuwayama, M., Shime, H., Machii, T., Kanakura, Y., Meyers, G., Wittwer, C., Chen, Z., Babcock, W., Frei-Lahr, D., Parker, C.J. & Kinoshita, T. (2006) Molecular basis of clonal expansion of hematopoiesis in 2 patients with paroxysmal nocturnal hemoglobinuria (PNH). *Blood*, **108**, 4232–4236.

Kitamura, T., Koshino, Y., Shibata, F., Oki, T., Nakajima, H., Nosaka, T. & Kumagai, H. (2003) Retrovirus-mediated gene transfer and expression cloning: powerful tools in functional genomics. *Experimental Hematology*, **31**, 1007–1014.

Mayr, C., Hemann, M.T. & Bartel, D.P. (2007) Disrupting the pairing between let-7 and Hmga2 enhances oncogenic transformation. *Science*, **315**, 1576–1579.

Noro, B., Licheri, B., Sgarra, R., Rustighi, A., Tessari, M.A., Chau, K.Y., Ono, S.J., Giancotti, V. & Manfioletti, G. (2003) Molecular dissection of the architectural transcription factor HMGA2. *Biochemistry*, **42**, 4569–4577.

Rotoli, B. & Luzzatto, L. (1989) Paroxysmal nocturnal hemoglobinuria. *Seminars in Hematology*, **26**, 201–207.

Takeda, J., Miyata, T., Kawagoe, K., Iida, Y., Endo, Y., Fujita, T., Takahashi, M., Kitani, T. & Kinoshita, T. (1993) Deficiency of the GPI anchor caused by a somatic mutation of the PIG-A gene in paroxysmal nocturnal hemoglobinuria. *Cell*, **73**, 703–711.

Tessari, M.A., Gostissa, M., Altamura, S., Sgarra, R., Rustighi, A., Salvagno, C., Caretti, G., Imbriano, C., Mantovani, R., Del Sal, G., Giancotti, V. & Manfioletti, G. (2003) Transcriptional activation of the cyclin A gene by the architectural transcription factor HMGA2. *Molecular and Cellular Biology*, **23**, 9104–9116.

Thuault, S., Valcourt, U., Petersen, M., Manfioletti, G., Heldin, C.H. & Moustakas, A. (2006) Transforming growth factor-beta employs HMGA2 to elicit epithelial-mesenchymal transition. *Journal of Cell Biology*, **174**, 175–183.

Vallone, D., Battista, S., Pierantoni, G.M., Fedele, M., Casalino, L., Santoro, M., Viglietto, G., Fusco, A. & Verde, P. (1997) Neoplastic transformation of rat thyroid cells requires the junB and fra-1 gene induction which is dependent on the HMGI-C gene product. *EMBO Journal*, **16**, 5310–5321.

Biochemical and Biophysical Research Communications 419 (2012) 662–669

Contents lists available at SciVerse ScienceDirect

Biochemical and Biophysical Research Communications

journal homepage: www.elsevier.com/locate/ybbrc

Using peripheral blood circulating DNAs to detect CpG global methylation status and genetic mutations in patients with myelodysplastic syndrome

Chisako Iriyama [a], Akihiro Tomita [a,*], Hideaki Hoshino [a], Mizuho Adachi-Shirahata [a], Yoko Furukawa-Hibi [b], Kiyofumi Yamada [b], Hitoshi Kiyoi [a], Tomoki Naoe [a]

[a] Department of Hematology and Oncology, Nagoya University Graduate School of Medicine, Nagoya, Japan
[b] Department of Neuropsychopharmacology and Hospital Pharmacy, Nagoya University School of Medicine, Nagoya, Japan

ARTICLE INFO

Article history:
Received 7 February 2012
Available online 20 February 2012

Keywords:
MDS
Circulating DNA
Genetic mutations
Epigenetics
LINE-1
TET2

ABSTRACT

Myelodysplastic syndrome (MDS) is a hematopoietic stem cell disorder. Several genetic/epigenetic abnormalities are deeply associated with the pathogenesis of MDS. Although bone marrow (BM) aspiration is a common strategy to obtain MDS cells for evaluating their genetic/epigenetic abnormalities, BM aspiration is difficult to perform repeatedly to obtain serial samples because of pain and safety concerns. Here, we report that circulating cell-free DNAs from plasma and serum of patients with MDS can be used to detect genetic/epigenetic abnormalities. The plasma DNA concentration was found to be relatively high in patients with higher blast cell counts in BM, and accumulation of DNA fragments from mono-/di-nucleosomes was confirmed. Using serial peripheral blood (PB) samples from patients treated with hypomethylating agents, global methylation analysis using bisulfite pyrosequencing was performed at the specific CpG sites of the *LINE-1* promoter. The results confirmed a decrease of the methylation percentage after treatment with azacitidine (days 3–9) using DNAs from plasma, serum, and PB mononuclear cells (PBMNC). Plasma DNA tends to show more rapid change at days 3 and 6 compared with serum DNA and PBMNC. Furthermore, the *TET2* gene mutation in DNAs from plasma, serum, and BM cells was quantitated by pyrosequencing analysis. The existence ratio of mutated genes in plasma and serum DNA showed almost equivalent level with that in the CD34+/38- stem cell population in BM. These data suggest that genetic/epigenetic analyses using PB circulating DNA can be a safer and painless alternative to using BM cells.

1. Introduction

Myelodysplastic syndrome (MDS) is one of the hematopoietic stem cell disorders, showing the features of dysplasia and a high rate of progression to acute myeloid leukemia (AML). Recent reports using next generation DNA sequencing techniques and single nuclear polymorphism (SNP) array analyses have suggested that specific gene mutations, resulting in aberrant DNA methylation [1], histone modification [2], and RNA splicing [3], may contribute to the pathogenesis of MDS. Furthermore, it is also speculated that an aberrant methylation status in some specific gene promoters [4,5] also contributes to pathogenesis and disease progression [6].

DNA hypomethylating reagents such as azacitidine and decitabine, known to be DNA methyltransferase inhibitors (DNMTi) [7], have recently come to be considered as standard therapeutics for patients with MDS [8]. Although DNMTi provide improvement of cytopenia and reduction of blast counts for certain patients, biomarkers, such as genetic mutations and methylation status of specific promoters, that predict the effectiveness of DNMTi before and/or during treatment, are still unclear. So far, cytogenetic and molecular analyses using bone marrow (BM) cells are the standard strategies for confirming the disease status of MDS; however, a disadvantage is that patients hesitate the performance of repeated BM aspiration because the procedure is more painful than peripheral blood (PB) aspiration. It is therefore highly desirable to find alternative strategies for detecting the serial genetic/epigenetic alterations those occur in BM cells.

Recently, circulating cell-free nucleic acids in the plasma and serum of PB, such as genomic DNA, mRNA, and microRNA, are recognized as useful materials for the detection of genetic/epigenetic abnormalities in malignant cells especially in patients who have solid tumors [9]. Previous reports suggest that a higher concentration of these nucleic acids correlates with disease progression or a higher tumor burden of solid tumors [10]. Furthermore, specific genetic mutations and epigenetic abnormalities including DNA methylation in solid tumors are also detectable by using circulating nucleic acids [9]. Circulating nucleic acids are expected to be

* Corresponding author. Address: Department of Hematology and Oncology, Nagoya University Graduate School of Medicine, Tsurumai-cho 65, Showa-ku, Nagoya 466-8550, Japan. Fax: +81 52 744 2161.
E-mail address: atomita@med.nagoya-u.ac.jp (A. Tomita).

0006-291X/$ - see front matter © 2012 Elsevier Inc. All rights reserved.
doi:10.1016/j.bbrc.2012.02.071

good materials for determining tumor status without performing re-operations or re-biopsies.

This report aims to show the usefulness of PB circulating DNAs for genetic/epigenetic analyses in patients with MDS. Plasma and serum circulating DNAs were obtained repeatedly from patients' PB after the administration of DNMTi. Serial changes of global DNA methylation status were successfully confirmed by using bisulfite pyrosequencing analysis. We propose that analysis using circulating DNAs can be a safer and painless alternate strategy compared to repeated BM aspiration for determining the genetic and epigenetic events in BM cells.

2. Materials and methods

2.1. Patients

Five patients with MDS in Nagoya University Hospital were enrolled into this analysis after obtaining appropriate informed consent. Patient UPN1 was a 74-year-old male who was diagnosed with MDS refractory anemia with excess blasts (RAEB)-1 by the World Health Organization (WHO) classification. He died after three courses of therapy with a demethylating agent because of disease progression to acute myeloid leukemia (AML). UPN2 was a 75-year-old male who was diagnosed as chronic myelomonocytic leukemia. He died at day 9 after the first course of azacitidine treatment (5 days) because of severe pulmonary bleeding originating from a background of autoimmunity. UPN3 was 74-year-old male who was diagnosed with MDS RAEB-2, and received azacitidine for 5 days, every 4 weeks. UPN4 was 65-year-old male diagnosed with MDS RAEB-t/AML, and received azacitidine for 7 days, every 4 weeks. UPN5 was 77-year-old female diagnosed with MDS refractory cytopenia with multilineage dysplasia, who received therapy with a demethylating agent and achieved complete remission.

2.2. Preparation of serum, plasma, and MNC from PB and BM of MDS patients

PB was drawn and placed into plain tubes with a separating agent for serum, and tubes with sodium ethylenediaminetetraacetate or heparin for plasma. Plasma and serum were aliquoted into 1.5 mL tubes after centrifugation at 415*g* or 1660*g* for 10 min at room temperature, and stored at −80 °C until genetic analysis. PBMNC and BM cells were collected using Ficoll paque [11].

2.3. DNA extraction

Genomic DNAs from PBMNC and BM cells were extracted using the QIAamp DNA Blood Mini Kit (QIAGEN, Valencia, CA). Circulating DNAs in plasma and serum (450 μL each) were extracted using MinElute Virus Vacuum Kit (QIAGEN) according to the manufacturer's instructions.

2.4. DNA methylation analysis with the bisulfite pyrosequencing strategy

Bisulfite conversion of genomic or circulating DNAs was performed using MethylEasy Xceed Rapid DNA Bisulphite Modification Kit (Takara, Ohtsu, Japan). DNA (15–300 ng) was utilized for one assay of conversion. For the polymerase chain reaction (PCR) for the analysis of *long interspersed nuclear elements-1* (*LINE-1*) (GenBank; X58075), the following primers were used, as indicated previously [12]: LINE-1-F; 5′-TTTTGAGTTAGGTGTGGGATATA-3′, and LINE-1-R; 5′-AAAATCAAAAAATTCCCTTTC-3′ with 5′ end biotinylation. PCR conditions were 95 °C for 30 s, 54 °C for 30 s, and 72 °C for 40 s for a total of 40 cycles. The PCR products were purified and single stranded with the PyroMark Vacuum Workstation according to the manufacturer's protocol and analyzed by the PSQ96MA Pyrosequencing System (QIAGEN) [12]. The primer for the pyrosequencing of the *Line-1* PCR product was as follows: LINE-1-pyro; 5′-AGTTAGGTGTGGGATATAGT-3′ [12]. The ratio of methylation was calculated from the existence percentage of unmethylated and methylated cytosines, indicated as thymine and cytosine. The methylation status for each sample was analyzed at least twice, and the results were statistically evaluated.

2.5. Single nuclear polymorphism (SNP) array analysis

The SNP array was analyzed with BM DNA using the 250k_Nsp GeneChip-SNP (Affymetrix), as previously described [13].

2.6. Pyrosequencing analysis for TET2 mutation

The PCR primers for *TET2* exon 6 were as follows: TET2-Ex6-F; 5′-GGCTGCAGTGATTGTGATTC-3′, and TET2-Ex6-R; 5′-TTGGGCTTTCCTATCAGTGG-3′ with 5′ end biotinylation, with the following conditions: 95 °C for 15 s, 56 °C for 20 s, and 72 °C for 30 s for a total of 50 cycles. Sequencing analysis was performed by the ABI 310 genetic analyzer (Applied Biosystems, Foster City, CA) with the following sequencing primer; TET2-Ex6-F2; 5′-GTCTCTGGCTGACAAACTCT-3′. The existence percentage of the *TET2* mutation was measured by pyrosequencing analysis using the primer as follows; TET2-Ex6-pyro; 5′-AGTTAGGTGTGGGATATAGT-3′.

2.7. Cell sorting

BM cells were sorted into CD34(+)/CD38(−), CD34(+)/CD38(+), and CD34(−) subpopulations with the BD FACS Aria (Becton Dickinson, Franklin Lakes, NJ) using the anti-CD34 APC antibody (Becton Dickinson) and the anti-CD38 PE-Cy7 antibody (Becton Dickinson), as shown previously [14].

2.8. Statistical analysis

Using Prism version 5 software (Graph Pad Software, Inc., La Jolla, CA), differences in methylation and the mutation percentage were analyzed with two way repeated measure ANOVA and one-way factorial ANOVA, respectively. The *p* values were 2-tailed, and a *p*-value of less than .05 was considered statistically significant.

3. Results

3.1. Peripheral blood circulating DNAs in MDS patients

Peripheral blood circulating DNA from plasma and serum obtained from healthy volunteer donors (Fig. 1A, lanes 1–4, and B) and MDS patients (Fig. 1C, Patient UPN1 to UPN5) were visualized via agarose gel electrophoresis. These DNAs were all prepared from 450 μL of serum or plasma, and suspended in 30 μL of distilled water after DNA extraction. Twenty-five percent of the total obtained DNA was applied for each one lane of the electrophoresis. The DNA from healthy volunteers was confirmed in all lanes; the DNA concentration in serum was much higher than that in plasma (Fig. 1A, lanes S versus P). The circulating DNA showed the ladder pattern suggesting the fragmentation of genomic DNA by the effect of deoxyribonuclease against chromatinized genomic DNA [15], as reported previously [9]. The size of the DNA fragments, analyzed by BioMax 1D software (Kodak), supported this phenomenon showing the multiple numbers of 160–180 base pairs from mono-, di-nucleosomes, and so on.

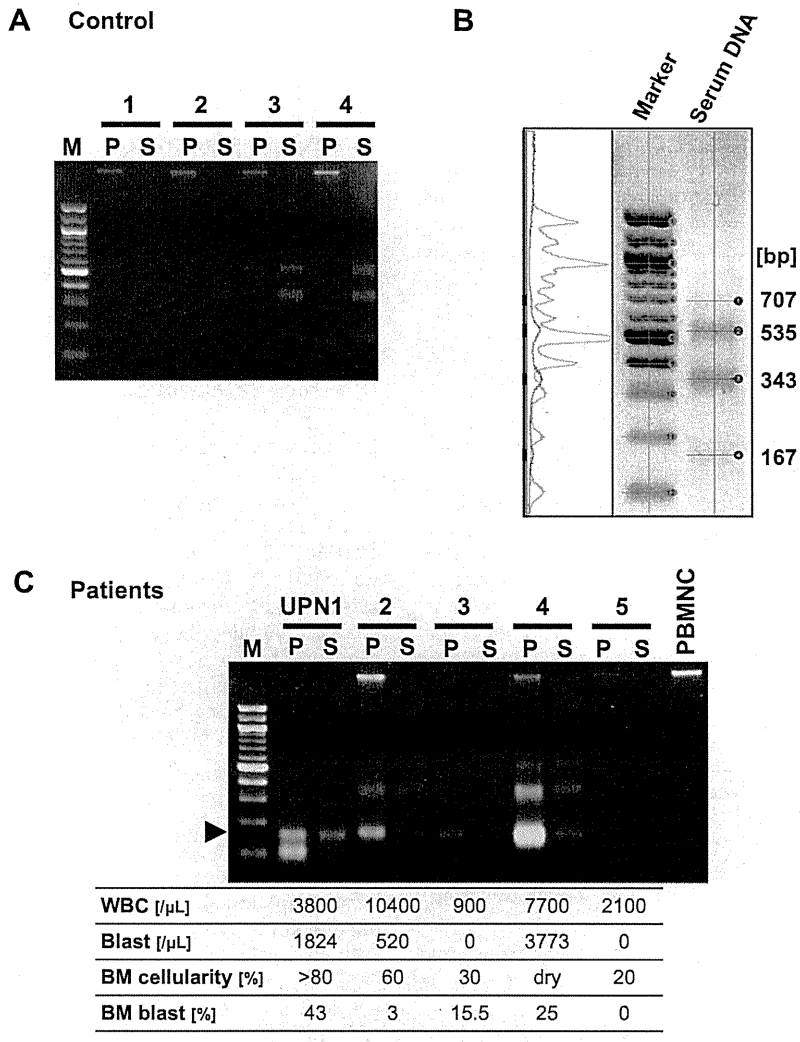

WBC [/μL]	3800	10400	900	7700	2100
Blast [/μL]	1824	520	0	3773	0
BM cellularity [%]	>80	60	30	dry	20
BM blast [%]	43	3	15.5	25	0

Fig. 1. Detection of peripheral blood circulating DNA from normal and MDS patients. (A) Circulating DNA from plasma (P) and serum (S) harvested from four healthy volunteer donors was visualized via agarose gel electrophoresis. DNA ladders were confirmed, especially with respect to serum DNA. Weak bands were confirmed also in plasma DNA after a longer exposure (data not shown). (B) DNA ladders were measured by DNA analysis software, and the size was calculated. The estimated band size of the serum DNA was indicated at the right side of the gel image. (C) Plasma and serum circulating DNAs were harvested from five MDS patients (UPN1–5) and visualized via agarose gel electrophoresis. The laboratory data for the white blood cells (WBC) and the blast cell count in PB and BM are also indicated in the bottom panel. Note that the DNA concentration of the plasma DNA was higher in some patients who had higher blast counts in their bone marrow cells. M: 100 bp DNA ladder marker.

When using the samples from the patients with MDS, the DNA concentration in the plasma was relatively higher than that in the serum; and the concentration seemed to parallel the amount of tumor (blast) cells in the BM and peripheral blood (Fig. 1C, Patient UPN1, 2, and 4). In these patients, DNA fragments from mononucleosome were relatively accumulated (the black triangle in Fig. 1C), and further digestion of the DNA was confirmed in one patient (UPN1, P). The total amount of the DNA from 1 mL of plasma or serum varied from 1.40 to 141 μg. The genomic DNA was obtained from PBMNC and also loaded into the gel electrophoresis.

These data suggest that the circulating DNAs from plasma and serum are also confirmed in MDS patients. The concentration of the plasma DNA may tend to reflect the blast cell amounts in the BM cells.

3.2. *Analysis of* LINE-1 *methylation in plasma and serum circulating DNAs*

LINE-1 are repeated sequences that exist in the amount of about 85,000 copies in normal cells. *LINE-1* are moderately rich in CpG sites. Most methylated CpGs are located in the 5′ region of the sequence that can function as an internal promoter [9]. Recent reports indicate that the methylation status of the CpG sites reflects the global methylation status, and that aberrant hypomethylation of these sites may correlate with malignant tumor biology [12,16].

We performed bisulfite pyrosequencing analysis for four CpG sites of the *LINE-1* promoter (Fig. 2A) using plasma and serum circulating DNA to confirm the usefulness of those DNAs to determine the global methylation status in MDS patients. Plasma, serum and MNC were obtained from UPN2 at days 1, 4 and 6 after starting the first course of azacitidine treatment, and the *LINE-1* methylation percentage was confirmed. The methylation percentage of each CpG site generally decreased after started the azacitidine treatment (Fig. 2B). Next, the average methylation ratio of all four CpG sites was confirmed. The methylation percentage at day 1 (untreated) was adjusted as 1, and the relative methylation rates at days 4 and 6 were calculated (Fig. 2C). In this assay, the demethylation effect produced by azacitidine on the *LINE-1* element was confirmed in PBMNC and plasma at day 6 and also confirmed in

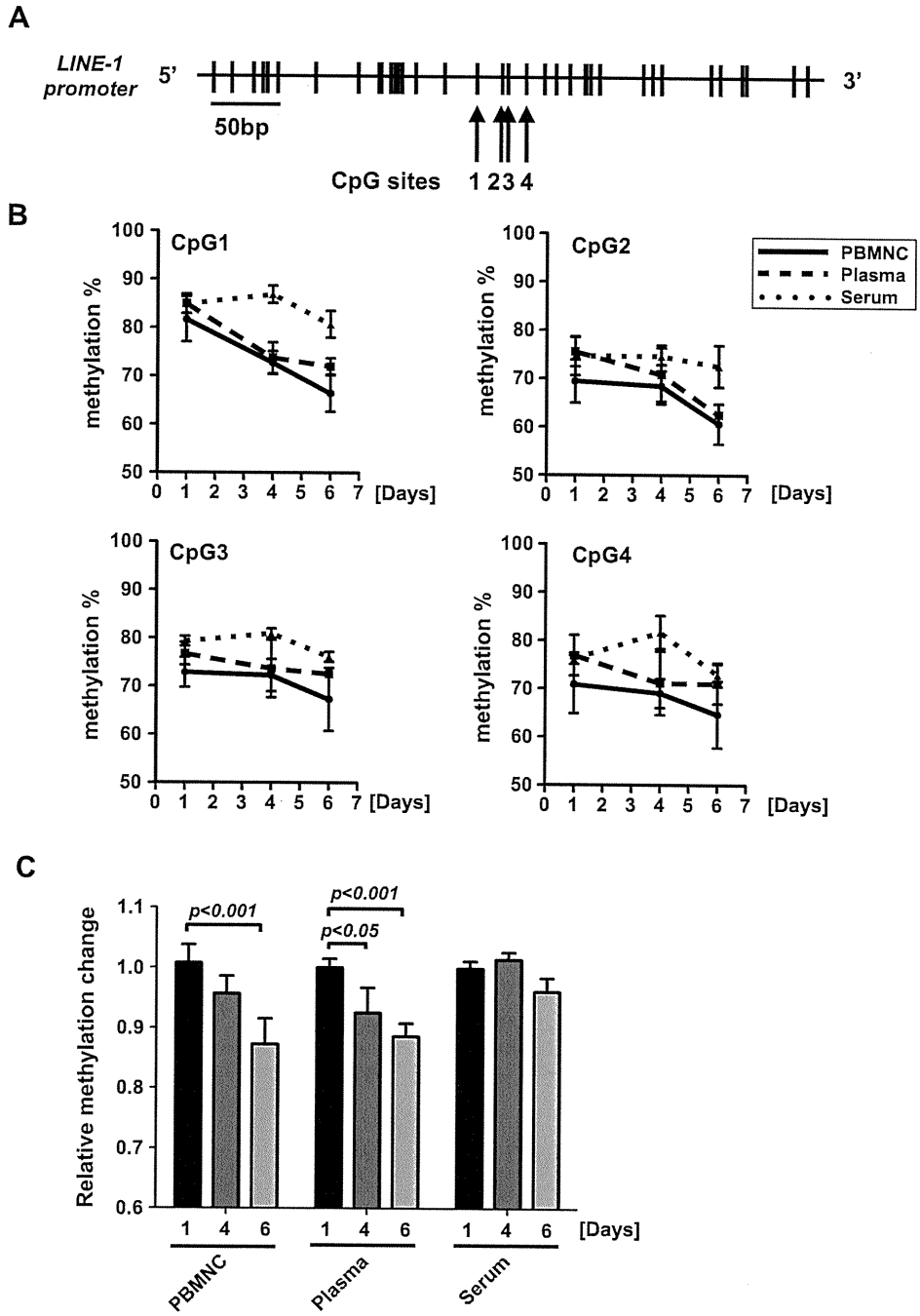

Fig. 2. *LINE-1* promoter CpG methylation status in a MDS patient treated with hypomethylating agent can be measured by using circulating DNAs. (A) Schematic representation of the *LINE-1* promoter CpG sites (GenBank; X58075, nucleotide position 108–520, complementary strand). Four CpG sites (1–4) were selected to measure cytosine methylation status by bisulfite pyrosequencing. (B) Peripheral blood was obtained from MDS UPN2 during the first azacitidine treatment cycle at days 1, 4, and 6. DNAs were prepared from plasma, serum, and PBMNC, and the methylation percentage of the four sites (CpG1–4) was quantitated by pyrosequencing analysis. The percentage of the methylation generally decreased after treatment with azacitidine. (C) The changing ratio of the methylation of all four sites was calculated using DNAs from PBMNC, plasma and serum, and the mean changing ratio was indicated in the bar graphs with the mean standard deviation (S.D.). The *p*-value was also indicated if the differences were significant.

plasma at day 4. In PBMNC, the tendency toward a decrease of the methylation ratio can be seen also at day 4, but was not significant. These data suggest that circulating DNA from plasma can be used for global methylation analysis with analysis of the *LINE-1* promoter as an alternative strategy using MNC in peripheral blood and/or BM.

3.3. Longer follow up of the global methylation status after treatment with a demethylating agent using plasma and serum circulating DNAs

Almost the same analysis was performed using peripheral blood samples from UPN4. PB was harvested 7 and 5 times during azacitidine treatment cycles 1 and 2 (Fig. 3A) and analyzed. The global

methylation ratio at the four CpG sites of the *LINE-1* elements generally decreased after starting treatment until day 9, and then increased again until the next treatment was started (days 12–28). To determine which samples of DNA were suitable for detection of the changing ratio after administration of azacitidine, the average methylation percentage of those four CpG sites was calculated using the data from days 1 to 9 in the first azacitidine course (Fig. 3B). In this assay, all DNA samples from PBMNC, plasma, and serum could detect the significant change of methylation status after azacitidine treatment. In particular, in this assay, plasma circulating DNA could detect the change much earlier at day 3 than DNA from PBMNC and serum. These data suggest that repeated sample collection from MDS patients can provide more accurate information about methylation status, and the methylation ratio of the *LINE-1* elements can be measured by using DNA circulating in the peripheral blood. Furthermore, taken together with the data of DNA concentration as shown in Fig. 1C, it is suggested that the DNA in plasma may be much more sensitive for detecting the change of methylation status in the blast cells in MDS patients.

3.4. Detection of genetic mutation using peripheral blood circulating DNAs

To test whether circulating DNAs can also be used for the detection of genetic mutations in MDS cells, mutation analysis was performed using plasma and serum circulating DNAs. BM cells from UPN1, showing 4q uni-parental disomy (UPD) by a SNP array (Fig. 4A), were utilized for genetic mutation analysis for the *TET2* gene. A non-sense point mutation of the *TET2* gene in exon 6, resulting in C-terminus truncation at the cysteine rich domain (CRD), was confirmed (Fig. 4B and C). Next, we performed pyrosequencing analysis to show the existence ratio of the *TET2* mutation

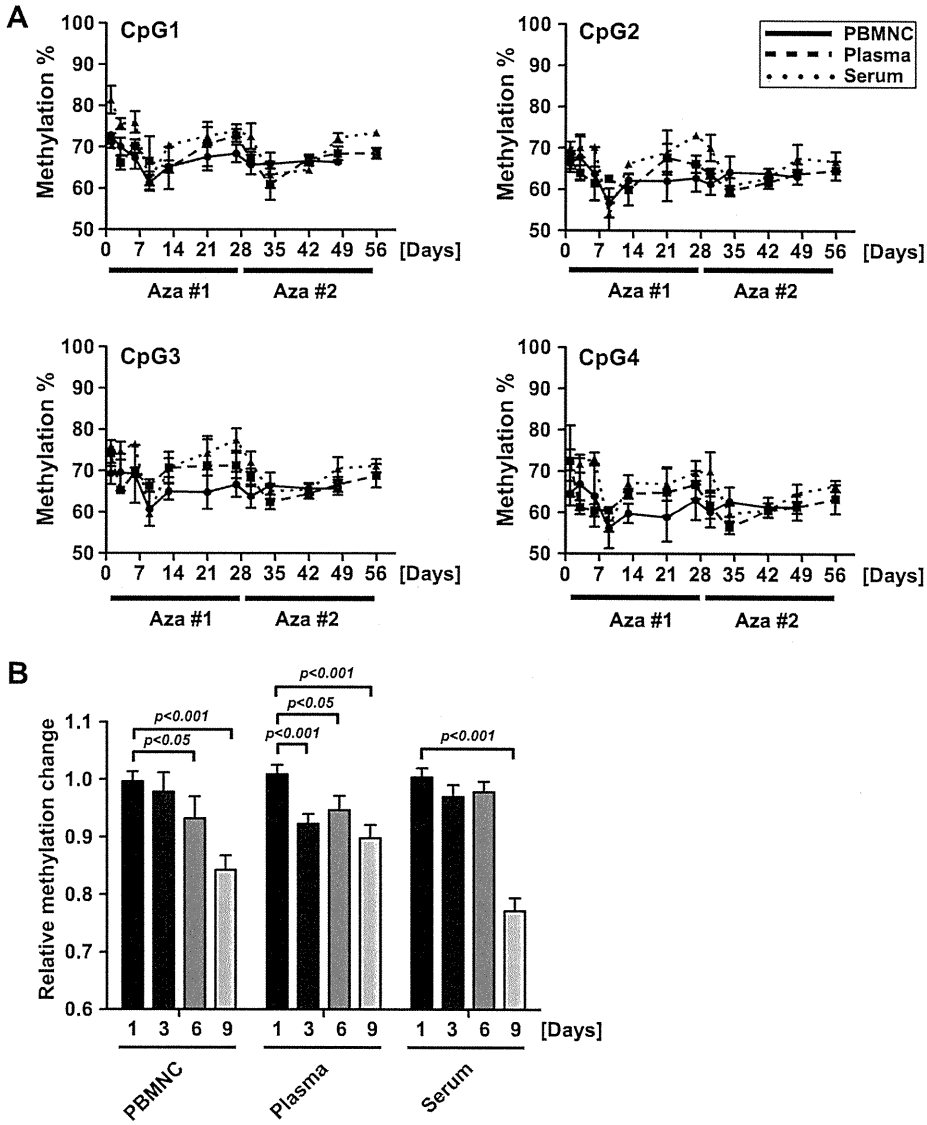

Fig. 3. A longer follow up of the *LINE-1* promoter CpG methylation status in an MDS patient treated with a hypomethylating agent using circulating DNAs. (A) Peripheral blood was obtained from MDS UPN4 during the first (#1) and the second (#2) azacitidine treatment cycle as indicated. DNAs were prepared from plasma, serum, and PBMNC, and the methylation percentage of the four sites (CpG1–4) was quantitated as analyzed in Fig. 2. Note that the methylation percentage was generally decreased until day 9, and the ratio was reversed until the next azacitidine treatment was started. (B) The mean changing ratio of the methylation of all four sites was calculated using DNAs from PBMNC, plasma, and serum, as analyzed in Fig. 2C.

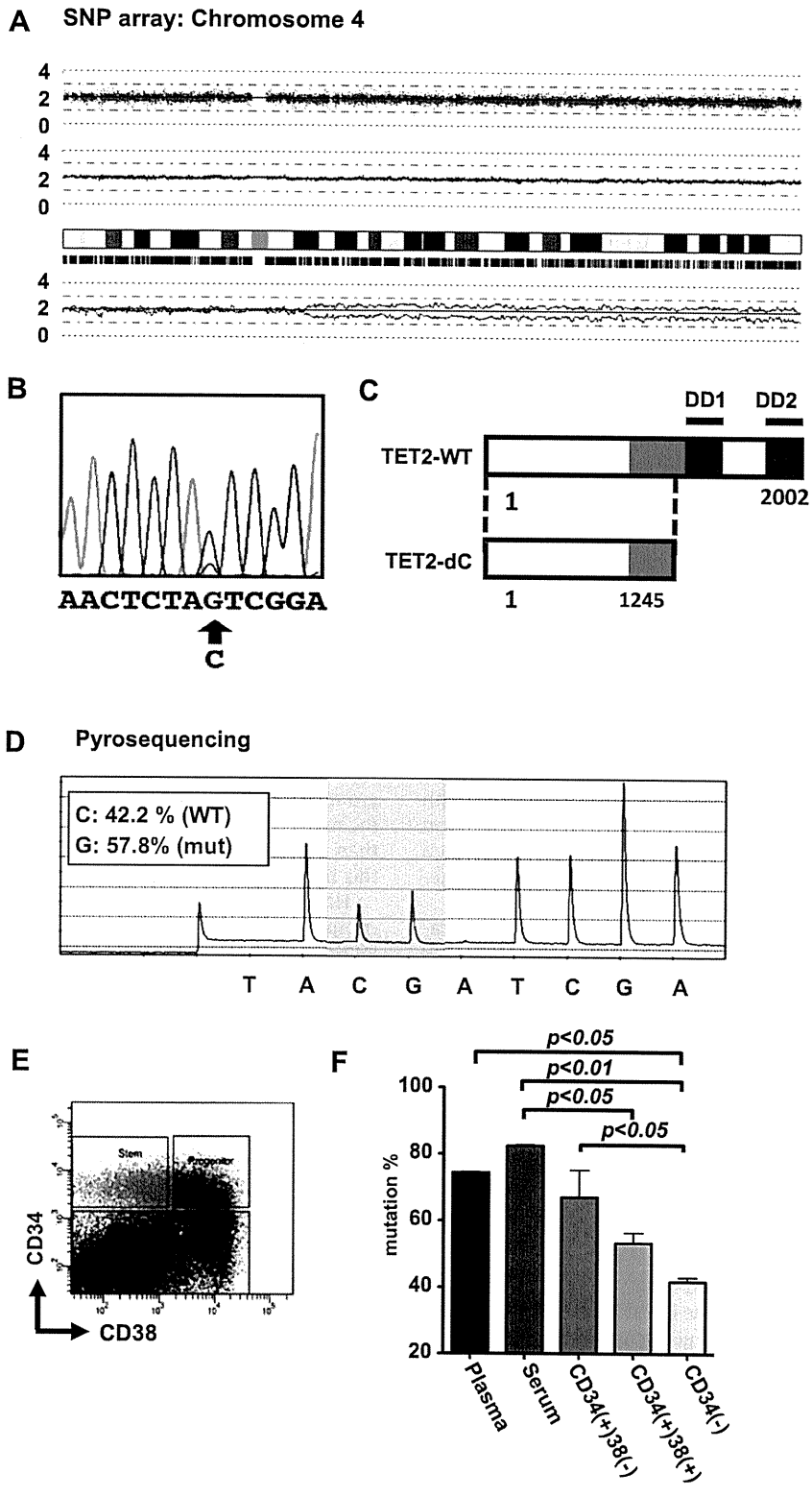

Fig. 4. Detection of the genetic mutations in an MDS patient using peripheral blood circulating DNAs. (A) SNP array analysis of UPN1. The DNA copy numbers were indicated on the green and red lines. UPD was observed in chromosome 4q. (B) Non-sense point mutation in the *TET2* gene exon 6, from TAC (tyrosine) to TAG (stop), was confirmed by the dye-terminator method. (C) Functional domains of wild-type TET2 and the putative C-terminally truncated TET2 protein (TET2-dC) in UPN1. CRD: cysteine rich domain, DD: dioxygenase domain. (D) Pyrosequencing analysis for the mutated region of the *TET2* gene using BM cells. The existence percentage of the wild-type (blue) and mutated (red) nucleotide was calculated by analyzing software. (E) BM cells of UPN1 were sorted into three subpopulations: CD34+/CD38− (stem), CD34+/CD38+(progenitor), and CD34− (others). (F) The existence ratio of the *TET2* mutation in each DNA prepared from circulating DNA (plasma and serum) and BM cell subpopulations (CD34+/CD38−, CD34+/CD38+, and CD34−).

using genomic DNA from whole BM cells of this patient. This mutation was detected by this assay indicating 57.8% of mutated clones. Since the mutation can be observed in both alleles in one cell (UPD), it was suggested that the wild type sequence came from the normal component of the patient.

To confirm whether the *TET2* mutation can also be detected in circulating DNA, and if so, whether the existing ratio of the mutation in circulating DNAs is much higher than that in components of BM cells, especially in stem cell population, three sorted BM cell populations (stem: CD34+/38−, progenitors: CD34+/38+, and others: CD34−) were utilized for the *TET2* mutation analysis using the pyrosequencing strategy. BM and peripheral blood aspiration from this patient were carried out in the same day. DNAs from plasma, serum, and the three populations of BM cells (Fig. 4E) were prepared, and pyrosequencing analysis was performed to confirm the existence ratio of the mutated *TET2* gene. The result was that the existence ratio of the mutants was significantly higher in serum and plasma than that in CD34-negative BM cells (Fig. 4F). These results indicated that circulating DNAs from plasma and serum can be used for the detection of genetic mutations in MDS cells. Furthermore, these data also suggest that plasma and serum DNA may likely come from the MDS clones distributed in these three populations, especially in CD34+/38− population, which might be relatively more fragile than normal cells. Further investigation is required to prove this hypothesis.

4. Discussion

The aim of this study was to check whether peripheral blood circulating DNA is useful for the detection of disease specific genetic and epigenetic changes in patients with MDS. Because MDS usually shows relatively slow disease progression compared with acute leukemia, patients and clinicians tend to hesitate to perform BM aspiration repeatedly to estimate the disease status. Our data suggest that plasma and serum DNAs are able to be used for the genetic and epigenetic assays instead of BM cells.

Interestingly, our data suggest that the plasma DNA concentration tends to reflect BM blast counts (Fig. 1C). This finding may indicate that the PB circulating DNA may come from relatively fragile MDS cells rather than normal cells. If so, there is a possibility that abnormal DNAs from the MDS clone may be much more enriched in the circulating DNA compared with DNAs from BM or PBMNC. This hypothesis may also explain two of our results: (1) the methylation status can be decreased more rapidly in plasma DNA than in PBMNC, as shown in Figs. 2C and 3B, (2) the existence ratio of the genetic mutation in plasma and serum DNA is relatively higher than that in the BM cells. A large number of patients are needed to confirm this phenomenon.

As shown in Fig. 1C, a higher concentration of digested DNA fragments, especially the accumulation of DNA fragments from mono-nucleosomes, can be observed in MDS patients who may have a relatively higher tumor volume in BM. Since the fragmentation of the DNA in the chromatin structure can occur through the enzymatic activity of deoxyribo-nuclease I (DNase I), a higher degree of enzymatic activity in plasma may serve as a biomarker that shows disease activity in MDS. Interestingly, further digestion of DNA fragments from one nucleosome structure (~200 bp) could be observed in UPN1 (Fig. 1C). This fragmentation could not be observed when we used the plasma sample after several freeze and thaw treatments (data not shown). This may indicate that some other DNase activity in specific patients correlates with this phenomenon. Further investigation is needed.

In our experiments, the plasma circulating DNA concentration of MDS patients was much higher than that in serum. An explanation for this phenomenon may be that many DNA fragments can be absorbed into blood clots after collection into sample tubes. The difference between the DNA concentrations in plasma and serum may correlate with the phenomenon that plasma DNA, compared with serum DNA, tends to more effectively detect the epigenetic changes in MDS cells (Figs. 2 and 3). These findings indicate that circulating DNA from plasma is better suited for epigenetic analysis than that from serum in MDS patients.

For detection of the CpG methylation status of specific gene promoters, we analyzed the methylation status of the $p15^{INK4B}$ promoter, known to be one of the hypermethylated genes in MDS patients [4,17]. Unfortunately, the result did not seem to be accurate with relatively varied data among the repeated experiments, even when using plasma DNA and nested PCR technique (data not shown). One possibility is that the DNA concentration was not sufficient for the bisulfite sequencing analysis. In contrast, the result of the *LINE-1* methylation (Figs. 2 and 3) was much more reliable compared with the analysis for the $p15^{INK4B}$ gene, because of the sufficient number of DNA copies for the *LINE-1* promoter: ~85,000 copies for *LINE-1* versus only two copies for the $p15^{INK4B}$ gene in one cell. From this standpoint, DNA methylation analysis focusing on the *LINE-1* promoter using plasma circulating DNA may be a good strategy to confirm the global methylation status in MDS patients.

Interestingly, an experiment for UPN4 indicated that the decreasing ratio of DNA methylation of the *LINE-1* promoter after treatment with azacitidine was detected much earlier when using plasma DNA (Figs. 2C, day 4, and 3B, day 3) than when using PBMNC (Figs. 2C and 3B, day 6). Since DNMTi are incorporated into DNA (and RNA) during cell division, MDS/AML cells that have a more rapid cell division cycle compared with intact cells may be affected more quickly by DNMTi in BM. Furthermore, MDS clones have a more fragile character resulting from "dysplastic" backgrounds. Taking this into consideration, circulating DNA from plasma may better reflect the DNA that comes from MDS clones in BM than from intact cells. Further investigation is required to prove this hypothesis.

Harvesting PB is painless, and is a safer and easier procedure compared with obtaining BM cells. Preparing plasma is much easier than preparing PBMNC, and plasma can very easily be stored in tubes in the freezer. Utilization of plasma circulating DNA for MDS patients may provide a new way to analyze the serial genetic/epigenetic changes that are integral to an understanding of MDS pathogenesis and their disease condition.

Acknowledgments

This work was supported by Grants-in-Aid from the Ministry of Health, Labor and Welfare, and the Ministry of Education, Culture, Sports, Science and Technology, Japan. We thank Dr. Seishi Ogawa and Dr. Masashi Sanada for performing the SNP array analysis. We thank Chika Wakamatsu, Eriko Ushida, Yukie Konishi, Mari Otsuka, Manami Kira, Mirei Okamoto, and Rie Kojima for valuable laboratory assistance.

References

[1] M.J. Walter, L. Ding, D. Shen, J. Shao, M. Grillot, M. McLellan, R. Fulton, H. Schmidt, J. Kalicki-Veizer, M. O'Laughlin, C. Kandoth, J. Baty, P. Westervelt, J.F. DiPersio, E.R. Mardis, R.K. Wilson, T.J. Ley, T.A. Graubert, Recurrent DNMT3A mutations in patients with myelodysplastic syndromes, Leukemia 25 (2011) 1153–1158.

[2] T. Ernst, A.J. Chase, J. Score, C.E. Hidalgo-Curtis, et al., Inactivating mutations of the histone methyltransferase gene EZH2 in myeloid disorders, Nat. Genet. 42 (2010) 722–726.

[3] K. Yoshida, M. Sanada, Y. Shiraishi, et al., Frequent pathway mutations of splicing machinery in myelodysplasia, Nature 478 (2011) 64–69.

[4] M. Kim, B. Oh, S.Y. Kim, et al., P15INK4b methylation correlates with thrombocytopenia, blast percentage, and survival in myelodysplastic

syndromes in a dose dependent manner: quantitation using pyrosequencing study, Leuk. Res. 34 (2010) 718–722.
[5] J. Lin, Y.L. Wang, J. Qian, et al., Aberrant methylation of DNA-damage-inducible transcript 3 promoter is a common event in patients with myelodysplastic syndrome, Leuk. Res. 34 (2010) 991–994.
[6] L. Shen, H. Kantarjian, Y. Guo, et al., DNA methylation predicts survival and response to therapy in patients with myelodysplastic syndromes, J. Clin. Oncol. 28 (2010) 605–613.
[7] G. Egger, G. Liang, A. Aparicio, P.A. Jones, Epigenetics in human disease and prospects for epigenetic therapy, Nature 429 (2004) 457–463.
[8] G. Garcia-Manero, P. Fenaux, Hypomethylating agents and other novel strategies in myelodysplastic syndromes, J. Clin. Oncol. 29 (2011) 516–523.
[9] H. Schwarzenbach, D.S. Hoon, K. Pantel, Cell-free nucleic acids as biomarkers in cancer patients, Nat. Rev. Cancer 11 (2011) 426–437.
[10] D. Allen, A. Butt, D. Cahill, M. Wheeler, R. Popert, R. Swaminathan, Role of cell-free plasma DNA as a diagnostic marker for prostate cancer, Ann. NY Acad. Sci. 1022 (2004) 76–80.
[11] E. Goto, A. Tomita, F. Hayakawa, A. Atsumi, H. Kiyoi, T. Naoe, Missense mutations in PML-RARA critical for the lack of responsiveness to arsenic trioxide treatment, Blood 118 (2011) 1600–1609.
[12] F. Ohka, A. Natsume, K. Motomura, et al., The global DNA methylation surrogate LINE-1 methylation is correlated with MGMT promoter methylation and is a better prognostic factor for glioma, PLoS ONE 6 (2011) e23332.
[13] M. Sanada, T. Suzuki, L.Y. Shih, et al., Gain-of-function of mutated C-CBL tumour suppressor in myeloid neoplasms, Nature 460 (2009) 904–908.
[14] A. Abe, Y. Minami, F. Hayakawa, et al., Retention but significant reduction of BCR-ABL transcript in hematopoietic stem cells in chronic myelogenous leukemia after imatinib therapy, Int. J. Hematol. 88 (2008) 471–475.
[15] A.P. Wolffe, Transcriptional activation. Switched-on chromatin, Curr. Biol. 4 (1994) 525–528.
[16] K. Balassiano, S. Lima, M. Jenab, et al., Aberrant DNA methylation of cancer-associated genes in gastric cancer in the European Prospective Investigation into Cancer and Nutrition (EPIC-EURGAST), Cancer Lett. 311 (2011) 85–95.
[17] T. Uchida, T. Kinoshita, H. Nagai, et al., Hypermethylation of the p15INK4B gene in myelodysplastic syndromes, Blood 90 (1997) 1403–1409.

Frequent loss of HLA alleles associated with copy number-neutral 6pLOH in acquired aplastic anemia

*Takamasa Katagiri,[1,2] *Aiko Sato-Otsubo,[3] Koichi Kashiwase,[4,5] Satoko Morishima,[6] Yusuke Sato,[3] Yuka Mori,[3] Motohiro Kato,[3] Masashi Sanada,[3] Yasuo Morishima,[7] Kohei Hosokawa,[2] Yumi Sasaki,[2] Shigeki Ohtake,[1] †Seishi Ogawa,[3,5] and †Shinji Nakao,[2] on behalf of the Japan Marrow Donor Program

[1]Clinical Laboratory Science, Division of Health Sciences, and [2]Cellular Transplantation Biology, Kanazawa University Graduate School of Medical Science, Ishikawa, Japan; [3]Cancer Genomics Project, Graduate School of Medicine, University of Tokyo, Tokyo, Japan; [4]Tokyo Metropolitan Red Cross Blood Center, Tokyo, Japan; [5]Core Research for Evolutional Science and Technology, Exploratory Research for Advanced Technology, Japan Science and Technology Agency, Saitama, Japan; [6]Department of Hematology, Fujita Health University, Aichi, Japan; and [7]Department of Hematology and Cell Therapy, Aichi Cancer Center Hospital, Nagoya, Japan

Idiopathic aplastic anemia (AA) is a common cause of acquired BM failure. Although autoimmunity to hematopoietic progenitors is thought to be responsible for its pathogenesis, little is known about the molecular basis of this autoimmunity. Here we show that a substantial proportion of AA patients harbor clonal hematopoiesis characterized by the presence of acquired copy number-neutral loss of heterozygosity (CNN-LOH) of the 6p arms (6pLOH). The 6pLOH commonly involved the HLA locus, leading to loss of one HLA haplotype. Loss of HLA-A expression from multiple lineages of leukocytes was confirmed by flow cytometry in all 6pLOH(+) cases. Surprisingly, the missing HLA-alleles in 6pLOH(+) clones were conspicuously biased to particular alleles, including HLA-A*02:01, A*02:06, A*31:01, and B*40:02. A large-scale epidemiologic study on the HLA alleles of patients with various hematologic diseases revealed that the 4 HLA alleles were over-represented in the germline of AA patients. These findings indicate that the 6pLOH(+) hematopoiesis found in AA represents "escapes" hematopoiesis from the autoimmunity, which is mediated by cytotoxic T cells that target the relevant autoantigens presented on hematopoietic progenitors through these class I HLAs. Our results provide a novel insight into the genetic basis of the pathogenesis of AA. (*Blood.* 2011;118(25):6601-6609)

Introduction

Acquired aplastic anemia (AA) is a rare condition associated with BM failure and pancytopenia.[1] A series of classic observations and experiments have unequivocally supported that the autoimmunity to hematopoietic stem/progenitor cells (HSPCs) critically underlies the pathogenesis of the BM failure in the majority of AA cases. According to the widely accepted model of immune-mediated BM failure, activated cytotoxic T cells (CTLs) that recognize an auto-antigen(s) presented on HSPCs through their class I HLA molecules have a major role in initiating the autoimmune reactions.[2-4] However, no definitive evidence exists that supports this model or the presence of such CTL repertoires. Moreover, little information is available about their target antigens or about the way by which they are recognized by effector T cells.

Another long-standing issue on AA is its close relationship with clonal hematopoiesis.[5,6] It was first suspected from an apparent overlap between AA and paroxysmal nocturnal hemoglobinuria (PNH)[7,8] and was also implicated by the frequent development of late clonal disorders in AA, such as myelodysplastic syndromes, PNH, or even acute myeloid leukemia (AML).[9-11] Clonal hematopoiesis can be explicitly demonstrated by conventional clonality assays at presentation in a substantial proportion of newly diagnosed typical AA cases.[12] Although it has been expected that the inciting autoimmune insult somehow confers selective pressures on the evolution of clonal hematopoiesis,[5] the exact mechanism for such immunologic selection or escape is still unclear.

The objectives of this study, therefore, were to characterize the clonal nature of the hematopoiesis that is maintained even under the severe autoimmune insult in AA, and to explore the genetic/immunologic mechanism that could underlie the pathogenesis of AA. To achieve these aims, we performed single nucleotide polymorphism (SNP) array-based analysis of genomic copy numbers and/or allelic imbalances in peripheral blood (PB) specimens obtained from 306 patients with AA. Initially, we found that AA patients frequently showed clonal/oligoclonal hematopoiesis that lost specific HLA alleles as a result of copy number-neutral loss of heterozygosity (CNN-LOH) of the 6p arms, which led us to further analyses of the contribution of 6pLOH(+) clones to residual hematopoiesis and a large-scale epidemiologic study on the HLA alleles that are over-represented in AA, involving a total of 6,613 transplants registered in the Japan Marrow Donor Program (JMDP).

Methods

Subjects

PB specimens from a total of 306 patients with AA were analyzed for the presence of genetic alterations using SNP arrays (see Figure 1). The clinical

Submitted July 1, 2011; accepted September 18, 2011. Prepublished online as *Blood* First Edition paper, September 30, 2011; DOI 10.1182/blood-2011-07-365189.

*T.K. and A.S.-O. contributed equally to this study.

†S. Ogawa and S.N. contributed equally to this study.

The online version of this article contains a data supplement.

The publication costs of this article were defrayed in part by page charge payment. Therefore, and solely to indicate this fact, this article is hereby marked "advertisement" in accordance with 18 USC section 1734.

Table 1. Patient characteristics

	Newly diagnosed (n = 107)	Previously treated (n = 199)
Median age at diagnosis, mo (range)	64 (9-88)	24 (2-80)
Sex, male/female, no.	58/49	110/89
Severity of AA at onset, no. (%) of patients		
Severe	79 (74)	185 (93)
Nonsevere	28 (26)	14 (7)
History, mo, median (range)	19 (0.1-251)	51 (0.1-372)
Past treatment, no. (%) of patients		
ATG + CsA	—	39 (20)
CsA alone	—	51 (26)
Anabolic steroid alone	—	13 (7)
Unknown*	—	96 (48)

ATG indicates antithymocyte globulin; CsA, cyclosporine A; and —, not applicable.

*Information regarding previous therapies of 96 cases (from Japan Marrow Donor Program) was unavailable.

characteristics of these patients are summarized in Table 1 and supplemental Table 1 (available on the *Blood* Web site; see the Supplemental Materials link at the top of the online article). Among the 306 patients, 107 were newly diagnosed and 199 were previously treated. Ninety-six patients received allogeneic BM transplantation from unrelated donors through the JMDP, and their HLA information was available from the JMDP. The other 210 were newly genotyped for HLA-A, -B, -C, -DRB1, -DQB1, and -DPB1 alleles as described elsewhere.[13] A total of 103 patients had been treated with anti–thymocyte globulin plus cyclosporine, cyclosporine alone, or anabolic steroids at the time of sampling. All patients and healthy persons provided their informed consent before sampling in accordance with the Declaration of Helsinki. The study protocol was approved by the ethics committee of the Graduate School of Medical Science, Kanazawa University and also by that of the Graduate School of Medicine, University of Tokyo.

Analysis of genomic copy numbers and detection of 6pLOH

Genomic copy numbers, as well as allele-specific copy numbers, were analyzed by using GeneChip 500K arrays (Affymetrix) as previously described.[14,15] Briefly, genomic DNA from AA patients and normal controls were analyzed on GeneChip 500K arrays separately. After adjusting several biases introduced during experiments, signal ratios of the corresponding probes between test (patient) and controls were calculated across the genome to obtain genome-wide copy numbers. Genetic lesions, including copy number gains and losses, as well as CNN-LOHs, were first detected using a hidden Markov model-based algorithm implemented in the CNAG software.[14,15] Known copy number variations were carefully excluded by referring to the Database of Genomic Variants (www.projects.tcag.ca/variation). CNN-LOH in 6p involving the HLA locus was more specifically and sensitively detected by statistically evaluating the mean differences in allele-specific copy numbers between heterozygous SNPs on 6p (N = ~ 1400) that were telomeric from the 5′-end of the HLA-A locus (rs1655927) and all non-6p heterozygous SNPs (N = ~ 105 000) using the Mann-Whitney *U* test with the R package (www.r-project.org). Possible false-positive findings arising from multiple testing involving the 306 samples were evaluated by maintaining the false discovery rate under 0.01 as previously described,[16] where the microarray data of 1000 JMDP donor specimens obtained from an ongoing whole genome association study (unpublished data) were used to calculate an empiric null distribution.[17,18]

Determination of the missing HLA alleles in 6pLOH(+) clones in patients with AA

The 500K SNP data of the 1800 JMDP donor-recipient pairs (JMDP dataset), together with their HLA genotyping information, was used to generate an HLA SNP haplotype table on the GeneChip 500K platform, which contains the consensus SNPs of the 3 major haplotypes (P1, P2, and P3) in Japanese subjects[18] and the SNP sequences of all observed HLA haplotypes complementary to P1 to P3 within the JMDP set (N = 1576; data not shown). To determine the missing HLA haplotype in each 6pLOH(+) patient, those "HLA" haplotypes were first selected from the aforementioned HLA haplotype table that were compatible with the observed HLA genotypes of that patient. Among these, a candidate haplotype was selected such that it contained the minimum number of SNPs that were incompatible with the patient's genotype. For each candidate haplotype, genomic copy numbers were inferred at the heterozygous SNPs along that haplotype using the circular binary segmentation algorithm,[19,20] which divided the haplotype into one or more discrete segments with different mean copy numbers. Finally, each copy number segment was thought to be "missing," when the alternative hypothesis (Ha: $S_i \neq \overline{S_i}$, for $^{\forall}_i$) was supported against the null hypothesis (H_0: $S_i = \overline{S_i}$, for $^{\forall}_i$) using the Wilcoxon signed rank test with a significance level of .05, where S_i represents the allele-specific copy number at the ith heterozygous SNP site within the segment of the candidate haplotype with $\overline{S_i}$ being the corresponding value for the complementary haplotype (supplemental Figure 1). Finally, for those HLA types that appeared more than 8 times among 6pLOH(+) cases, their contribution to the observed allelic loss of HLA haplotypes was evaluated by multivariate logistic regression analysis with stepwise backward selection

Flow cytometry

Heparinized PB and BM were collected from the patients at diagnosis and/or after treatment. HLA-A expression on granulocytes, monocytes, B and T cells, and BM $CD34^+$ cells was analyzed by flow cytometry using a FACSCanto II instrument (BD Biosciences) with the FlowJo 7.6.1 program (TreeStar). The monoclonal antibodies used for this study are provided in supplemental Table 2.

Human androgen receptor assay

The human androgen receptor gene was amplified from genomic DNA of 23 female patients, including 3 6pLOH(+) patients, as described by Ishiyama et al[21] with some modifications. Clonality was assessed using an "S value" as a marker of skewing in granulocytes and T lymphocytes.

Association of HLA types with AA

A total of 6613 patients who had received allogeneic BM transplantation through the JMDP between 1992 and 2008 were investigated to see whether the HLA alleles frequently missing in CNN-LOH in 6p with the development of AA could represent risk alleles for the development of AA. Thus, the frequencies of patients with each of the candidate risk alleles (HLA-A*31:01, B*40:02, A*02:01, and A*02:06) and those having none of these alleles were compared between 407 patients with AA and those with other hematopoietic disorders (1827 with AML, 1606 with acute lymphocytic leukemia, 1014 with chronic myeloid leukemia, 825 with myelodysplastic syndrome, 566 with non-Hodgkin lymphoma, and 368 with other hematopoietic neoplasms; supplemental Table 3) by calculating the Fisher *P* values in the corresponding 2 × 2 contingency tables.

Results

Genetic lesions in AA detected by SNP array analysis

After excluding known or suspected copy number variations, a total of 50 genetic lesions were identified in 46 of the 306 (15%) PB specimens of our AA case series (Table 1; Figure 1). Among these by far, the most conspicuous was the recurrent CNN-LOH involving the 6p arm, which was detected in 28 cases as a significant dissociation of allele-specific copy number graphs in 6p regions using a hidden Markov model–based algorithm implemented in the CNAG software[2,14,15] (Figure 2A-2B). Of particular interest was that all CNN-LOH in 6p commonly affected the HLA locus, causing a haploid loss of HLA alleles and uniparental HLA expression. In some cases, the breakpoint of the 6pLOH was

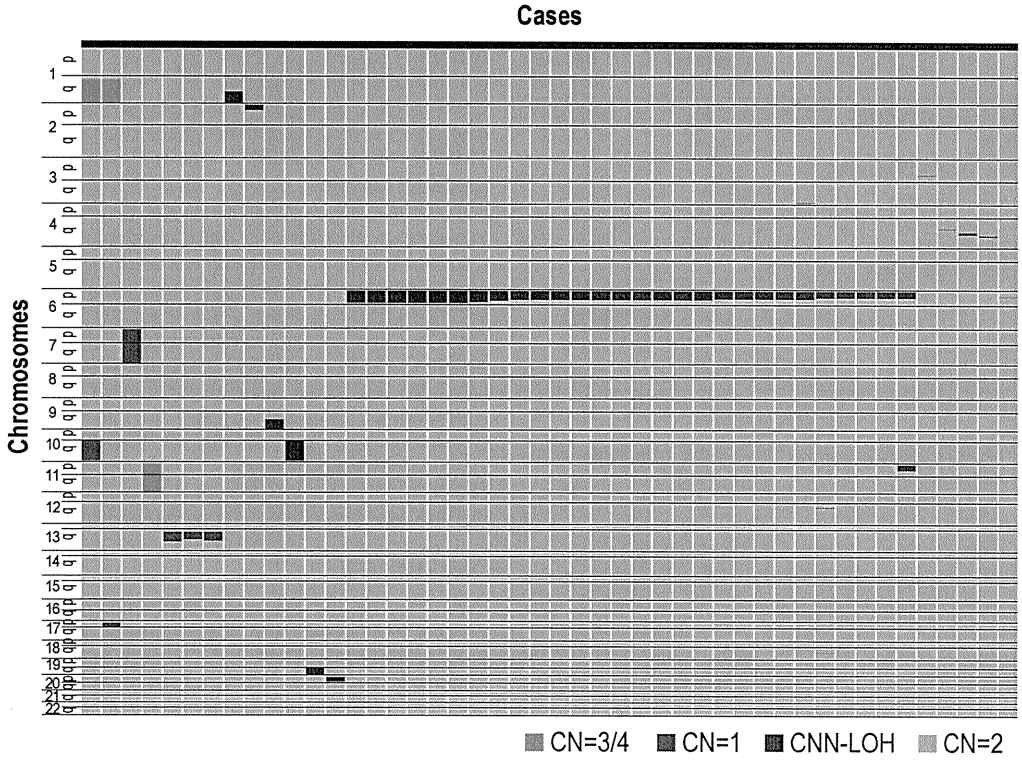

Figure 1. Copy number changes and allelic imbalances in 46 of the 306 AA cases. The copy number changes and allelic imbalances (or CNN-LOHs) in each case are summarized in the chromosomal order vertically for 46 AA cases with copy number abnormalities. Gains and losses, as well as CNN-LOHs, are shown in the indicated colors.

predicted to fall within the HLA locus (Figure 2B). These findings strongly indicated that the HLA locus was the genetic target of these 6pLOHs. Also supporting this was the finding that, in half of the cases, the dissociations in the allele-specific copy number graphs were gradually attenuated to the baseline over several mega base pair regions rather than showing a discrete breakpoint, indicating the presence of multiple 6pLOH(+) clones within a single case that had different breakpoints but still shared the same missing HLA alleles (Figure 2C). Moreover, the 6pUPDs existing only in a minor population were more sensitively detected by statistically evaluating the size of dissociation of allele-specific copy numbers in the 6p arm. With this improved statistical test, CNN-LOH in 6p was found in a total of 40 cases (13%; Figure 2D; supplemental Figure 2), where the false discovery rate was maintained at 0.01 to avoid too many false positive findings. In all 6pLOH(+) cases, substantial numbers of heterozygous SNP calls were retained within the affected regions, thus indicating that the CNN-LOHs in 6p were not constitutional but represented acquired genetic events only found in the affected subclones (Figure 1). Indeed, all 6pLOH(+) cases were shown to have "heterozygous" HLA alleles in high-resolution HLA typing of their PB (Table 2). Moreover, 6pLOH was not detected in the CD3-positive T cells in selected cases (cases 25 and 26, supplemental Figure 3). By quantitatively comparing the observed differences in allele-specific copy numbers in the 6pLOH segments with what were expected assuming 100% LOH(+) components, the 6pLOH(+) clones were estimated to account for 0.2% to 53.9% of the PB leukocytes (Table 2). The trend of the lower percentages of the 6pLOH(+) fraction in newly diagnosed patients compared with those in patients at remission was thought to reflect the fact that the former patients tended to have lower counts of granulocytes and monocytes, which were the predominant targets of 6pLOH (see supplemental Table 1).

The disease status of the 40 patients at the sampling was before treatment in 16 cases, during remission for 1 to 16 years after therapies in 15, and before BM transplantation for refractory disease in 9. All evaluable 6pLOH(+) AA cases responded to immunosuppressive therapy (IST) (23 of 23), whereas 101 of 126 evaluable cases with 6pLOH(−) responded ($P = .014$; Table 3).

Uniparental expression of HLA-A in multilineage hematopoietic cells

The genetic loss of one HLA haplotype in SNP array analysis was further confirmed by expression analysis of HLA-A in PB leukocytes using flow cytometry in 19 eligible cases with 6pLOH(+), in which the HLA-A alleles were heterozygous and fresh PB samples were available. Loss of expression of one HLA-A antigen was confirmed in all 19 6pLOH(+) cases (Figure 3A; supplemental Figure 4). The HLA-A missing cells in the PB were shown to have appeared shortly after the onset or before the initiation of treatments in 2 cases, and were confirmed to persist for 1 to 16 months (median, 6 months) in 14 patients (supplemental Table 1; supplemental Figure 5). The percentage of granulocytes lacking HLA-A antigens in the 2 patients who were responsive to IST remained almost the same during the convalescent period of 2 to 3 months (supplemental Figure 6). Importantly, uniparental expression of HLA-A alleles was detected in multiple cell lineages, including granulocytes, monocytes, B cells, and, to a lesser extent, in T cells. Moreover, uniparental HLA-A expression was demonstrated in BM $CD34^+$ cells in 5 patients whose BM samples were available for flow cytometry. All 5 patients possessed various proportions of BM $CD34^+$ cells (49.7%-71.3%), which had lost the expression of one

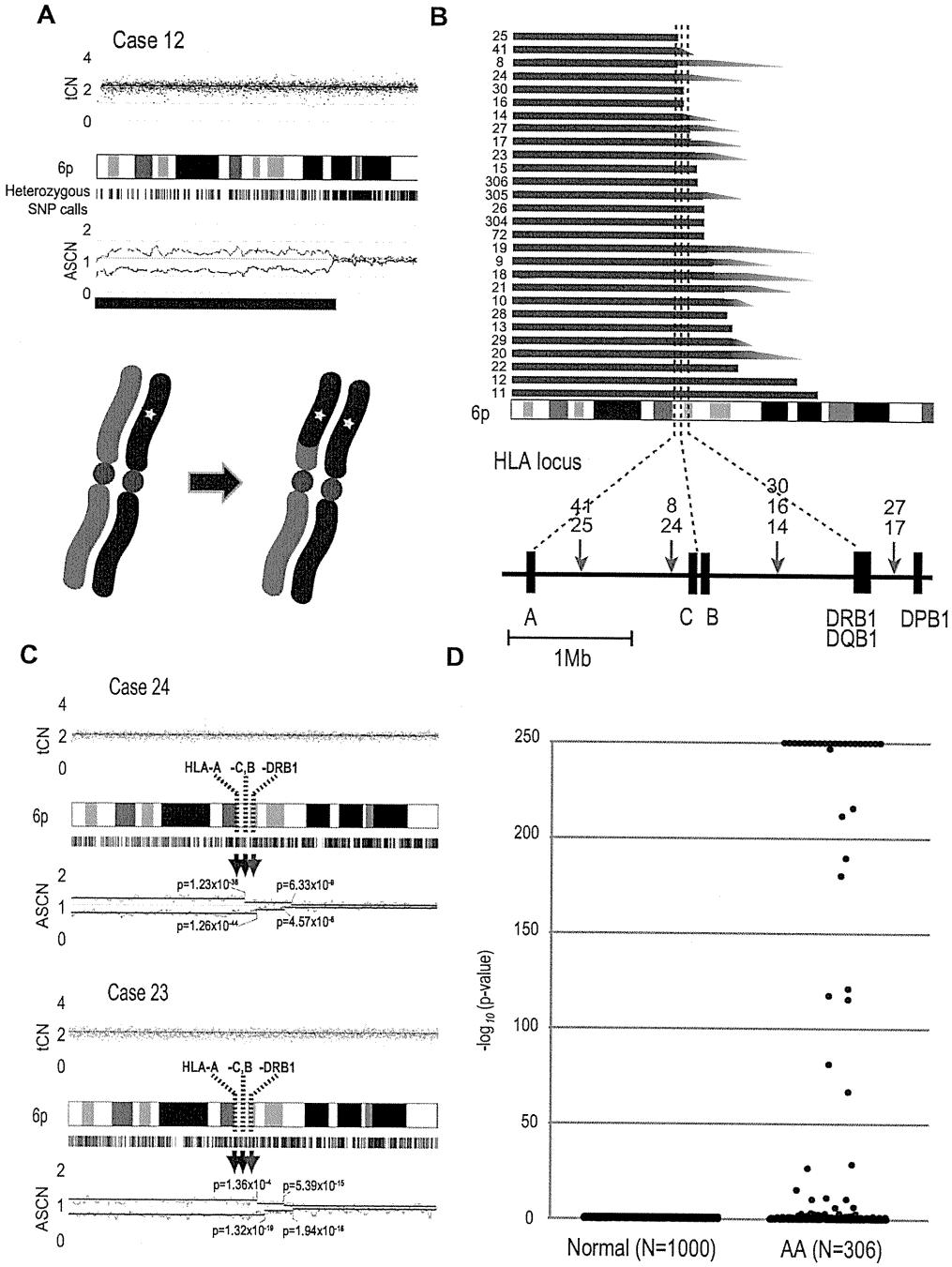

Figure 2. Acquired 6pLOHs in AA patients that target the HLA locus. (A) Typical CNAG outputs in SNP array analysis showing CNN-LOH (purple line) that appears as significant dissociation in allele-specific copy number graphs (red and green lines) from the baseline with normal total copy numbers (tCN; top panel). As a result of an allelic conversion, the affected segment causes LOH (* indicates 1; bottom panel). The "acquired" origin of these lesions is indicated by the retention of substantial numbers of heterozygous SNP calls (green bars below the chromatogram) that would otherwise mostly disappear. (B) The breakpoints of 6pLOHs found in a total of 28 AA cases, all involving the HLA locus in common. In more than half of cases (indicated by arrowheads in panel B), the exact location of the breakpoint was difficult to uniquely determine, where dissociation of the allele-specific copy number graphs continuously tapered along the 6p arm, indicating the presence of multiple 6pLOH(+) clones with common missing alleles (C). Indeed, the breakpoint containing regions are separated into multiple segments having significantly different copy numbers in the circular binary segmentation model, as indicated by solid lines with *P* values. Note that the most telomeric breakpoint is located within (case 24) or centromeric to (case 23) the HLA locus in each case. (D) A skewed distribution of the logarithm of *P* values in AA cases compared with normal persons. The *P* values were calculated in the Mann-Whitney *U* test, with which the difference in the mean allele-specific copy numbers between 6p and other chromosomal regions was evaluated (see "Analysis of genomic copy numbers and detection of 6pLOH"). A total of > 250 values are plotted as 250.

HLA-A antigen; and in each case, the missing HLA-A allele was identical to that in the PB leukocytes (Figure 3B). The uniparental expression of HLA-A in case 13 was also observed in the $CD34^+$ compartment of the archived BM specimen obtained 2 years before analysis (supplemental Figure 7). Together, these findings suggested that the 6pLOH involved early HSPCs and that the 6pLOH occurred at the level of long-term repopulating stem cells.

Table 2. 6pLOH(+) AA cases and imputed allelic status of HLA alleles

UID	6pUPD(+) fraction,* %	Missing alleles						Retained alleles					
		A	B	C	DRB1	DQB1	DPB1	A	B	C	DRB1	DQB1	DPB1
19	53.9	31:01††‡	40:02†	03:04†	12:01	03:01	05:01	24:02	52:01	12:02	15:02	06:01	05:01
12	51.8	02:01††‡	40:02†	03:03	15:01	06:02	05:01	26:02	40:06	08:01	09:01	03:03	05:01
17	51.6	24:02	13:01	03:04†	12:02	03:01	04:02	24:02	52:01	12:02	15:02	06:01	09:01
304	49.3	31:01††‡	55:02	01:02	12:02	03:01	41:01	24:02	07:02	07:02	01:01	05:01	04:02
11	48.0	02:06††‡	40:02†	03:04†	15:01	06:02	ND‖	11:01	67:01	07:02	16:02	05:02	ND‖
21	46.2	31:01‡§	51:01	14:02	14:05	05:03	03:01	24:02	07:02	07:02	01:01	05:01	04:02
24	44.9	31:01†	40:02†	03:04†	11:01	03:01	02:01	24:02	40:06	08:01	09:01	03:03	05:01
26	44.3	31:01††§	40:01	03:04†	04:05	04:01	03:01	26:03	52:01	12:02	15:02	06:01	09:01
27	43.5	02:06†	40:02†	03:04†	04:10	04:02	02:01	11:01	52:01	12:02	15:02	06:01	09:01
10	42.1	31:01†	40:02†	03:04†	08:03	06:01	02:01	24:02	51:01	14:02	09:01	03:03	02:01
8	40.8	02:06††‡	40:02†	03:03	12:01	03:01	05:01	24:02	52:01	12:02	15:02	06:01	04:02
23	35.2	02:01†	40:02†	03:04†	09:01	03:03	02:01	24:02	54:01	01:02	04:05	04:01	04:02
25	32.1	02:06††‡			No LOH			01:01			No LOH		
9	23.5	02:06††‡	39:01	07:02	08:02	04:02	02:01	24:02	15:18	07:04	04:01	03:01	14:01
20	21.7	26:01‡	40:02†	03:03	15:01	06:02	05:01	02:18	46:01	01:02	08:03	06:01	05:01
14	21.7	31:01††‡	51:01	14:02	09:01	03:03	05:01	24:02	52:01	12:02	15:02	06:01	09:01
22	20.6	02:01†	39:01	07:02	08:03	06:01	05:01	24:02	52:01	12:02	15:02	06:01	09:01
18	17.6	02:01††‡	40:06	08:01	09:01	03:03	02:01	24:02	35:01	03:03	15:01	06:02	04:02
15	17.4	02:06†	40:06	08:01	09:01	03:03	02:01	24:02	07:02	07:02	01:01	05:01	02:01
41	15.2†	31:01††‡	35:01	03:03	09:01	03:03	03:01	26:01	39:01	07:02	08:03	06:01	05:01
28	12.8	24:02	54:01	01:02	01:01	05:01	04:02	24:02	52:01	12:02	15:02	06:01	09:01
29	11.7	31:01†	40:02†	03:04†	15:01	06:02	02:01	24:02	54:01	01:02	04:05	04:01	05:01
305	10.3	02:06††‡	40:02†	15:02	15:02	06:01	04:01	24:02	51:01	14:02	09:01	03:03	02:01
13	9.6	24:02‡	40:02†	03:04†	15:01	06:02	02:01	02:01‡	35:01	08:01	09:01	03:03	02:01
306	8.5	24:02‡	40:02†	03:04†	09:01	03:03	02:01	26:02	40:06	08:01	09:01	03:03	02:01
16	8.1	11:01	40:06	08:01		No LOH		24:02	46:01	01:02		No LOH	
30	8.0	02:06†	39:01	07:02		No LOH		24:02	40:06	08:01		No LOH	
72	5.6	02:01†	40:02†	03:04†	09:01	03:03	05:01	02:07	46:01	01:02	08:03	06:01	02:02
36	4.0	02:01††‡	ND¶	ND#	15:02	06:01	09:01	24:02	ND¶	ND#	15:02	06:01	09:01
124	3.5	24:02	40:02†	03:04†	12:01	03:01	02:01	24:02	52:01	12:02	15:02	06:01	09:01
223	2.8	31:01††‡	48:01	03:04†	09:01	03:03	05:01	02:06†	39:01	07:02	15:01	06:02	02:01
215	2.8	31:01†	51:01	14:02	08:02	04:02	04:02	03:01	44:02	05:01	13:01	06:03	05:01
181	1.3	02:06†	13:01	03:04†	12:02	03:01	05:01	24:02	52:01	12:02	15:02	06:01	09:01
97	1.0	24:02	07:02	07:02	01:01	05:01	05:01	02:01†	39:01	07:02	15:01	06:02	02:01
252	0.9	ND**	40:02†	03:04†	09:01	03:03	05:01	ND**	46:01	01:02	04:05	04:01	05:01
118	0.9	02:06‡§	40:02†	03:04†	08:02	03:02	05:01	24:02	52:01	12:02	15:02	06:01	09:01
298	0.8	24:02	40:02†	03:04†	15:01	06:02	05:01	24:02	52:01	12:02	15:02	06:01	09:01
188	0.7	24:02	52:01	12:02	15:02	06:01	09:01	02:01†	52:01	12:02	11:01	03:01	05:01
291	0.7	31:01†	51:01	14:02	15:01	06:02	02:01	24:02	40:01	03:04†	11:01	03:01	05:01
196	0.2	ND†† (A*02:06/24:02, B*35:01/51:01, C*03:03/15:02, DRB1*04:03/15:01, DQB1*03:02/06:02, DPB1*0:201/02:01)											

UID indicates unique ID.
*The percentage of 6pUPD(+) fraction is derived from total peripheral blood leukocytes that include lymphoid as well as myeloid element.
†HLA types significantly deviated to missing alleles.
‡The allelic loss was confirmed by flow cytometry.
§The missing haplotype was determined by flow cytometry.
‖DPB1*04:02/05:01.
¶B*15:18/52:01.
#C*08:01/12:02.
**A*02:01/02:07.
††Missing allele was not determined because copy number changes in these segments were not statistically significant.

Clonality of the HLA-missing granulocytes

The human androgen receptor-based clonality assays in granulocytes were performed in 3 6pLOH(+) and 20 6pLOH(−) patients, in which all 3 6pLOH(+) and 4 (20%) of the 6pLOH(−) patients showed evidence of clonality in granulocyte populations (supplemental Figure 8).

Missing HLA alleles in 6pLOH

Given that the HLA is the genetic target of 6pLOH in AA, the missing HLA alleles in 6pLOH are of particular interest because in this context they are thought to be directly involved in the presentation of the target auto-antigens to CTLs and, therefore, to be critically important in the pathogenesis of AA. We determined the missing HLA alleles in each 6pLOH(+) AA patient by the haplotype imputation of HLA alleles based on the large data of HLA haplotypes observed in the JMDP set, followed by statistical evaluation of allele-specific copy numbers along the imputed haplotypes (Figure 4). The imputed haplotypes were confirmed in 4 cases by the family studies on the HLA. The allelic status was imputed at least partially in 39 of the 40 6pLOH(+) cases. The imputed results were consistent with the patterns of uniparental expression of HLA-A in flow cytometry in 18 cases with 6pLOH (Table 2; Figure 4), except for those in case 26, in which no valid SNP haplotype

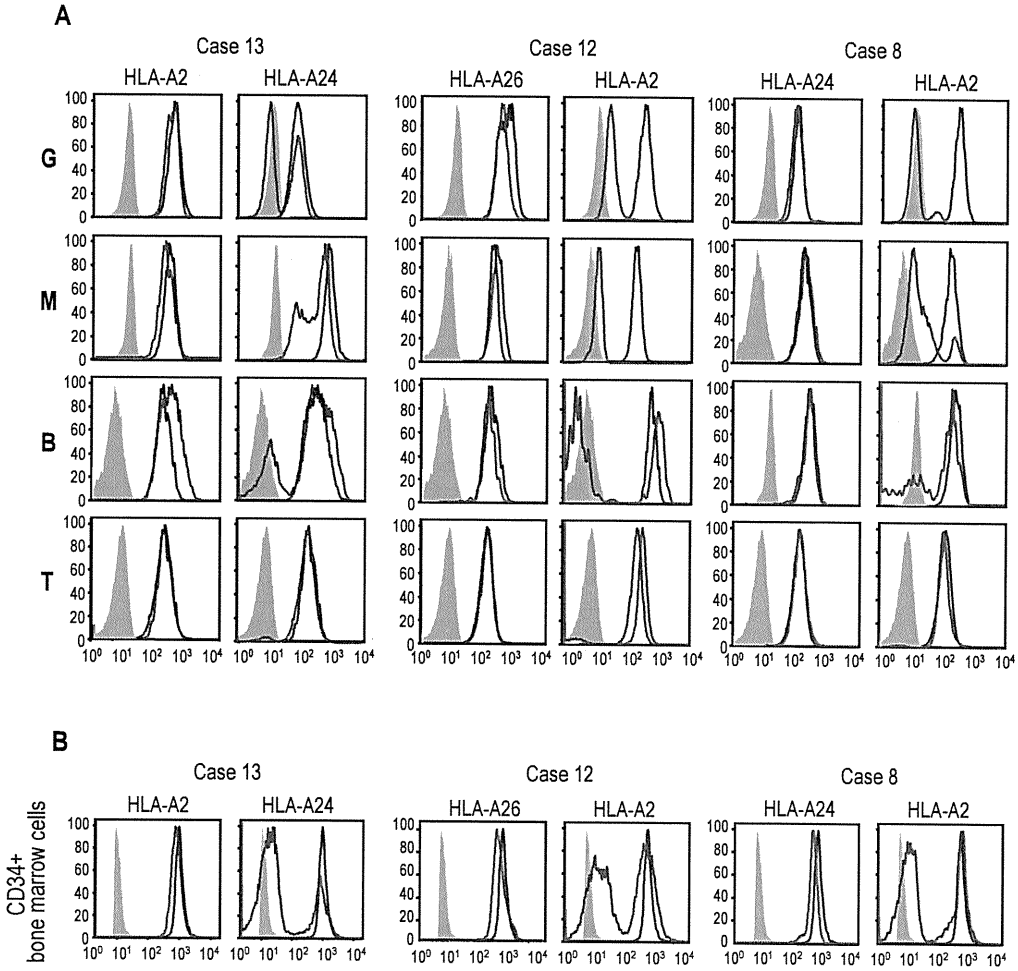

Figure 3. Uniparental expression of HLA in AA cases with CNN-LOH in 6p. Allele-specific expression of HLA-A antigens in AA specimens was examined by flow cytometry using monoclonal antibodies that specifically recognize the indicated HLA types (red lines), where leukocytes from healthy persons were used as a control (blue lines). (A-B) The uniparental expression of HLA-A antigens in PB leukocytes and BM CD34$^+$ cells obtained from 3 AA cases with CNN-LOH in 6p. Different leukocyte compartments were separately examined, including granulocytes (G), monocytes (M), B-lymphocytes (B), and T-lymphocytes (T).

around the HLA-A locus was identified and the status of HLA-A was determined by flow cytometry. The missing HLA alleles in 6pLOH(+) AA showed a conspicuous deviation to some selected HLA alleles, including HLA-A*31:01, B*40:02, C*03:04, and, to a lesser extent, HLA-A*02:01 and A*02:06. After the effects of linkage disequilibrium between individual HLA alleles were taken into consideration by multivariate analysis, 4 HLA alleles were shown to remain as the principal determinants of the missing haplotypes, HLA-A*31:01, B*40:02, A*02:01, and A*02:06 (supplemental Table 4).

Over-representation of frequently missing HLAs in AA populations

Because these missing HLA alleles in 6pLOH could be involved in the pathogenesis of AA, we next tested whether these relevant HLA alleles are associated with the risk of the development of AA among the 6,613 JMDP registrants. As shown in Table 4, the 4 major missing HLA alleles, HLA-A*31:01, B*40:02, A*02:01, and A*02:06, were more frequently observed in AA cases compared with nonsignificant HLA alleles (ie, all HLA alleles other

Table 3. Response rate (CR + PR) according to the Camitta criteria

	Newly diagnosed (n = 107)		Previously treated (n = 103)	
	6pLOH(−) (n = 91), no. (%)	6pLOH(+) (n = 16), no. (%)	6pLOH(−) (n = 88), no. (%)	6pLOH(+) (n = 15), no. (%)
Immunosuppressive therapies (all)	36/49 (73)	11/11 (100)	65/77 (84)	12/12 (100)
ATG + CsA	14/19 (74)	7/7 (100)	27/33 (82)	5/5 (100)
CsA alone	22/30 (73)	4/4 (100)	38/44 (86)	7/7 (100)
Anabolic steroid alone	0/0 (0)	0/0 (0)	7/11 (64)	2/2 (100)
Unknown/not evaluable	42	5	0	1

CR indicates complete remission; PR, partial remission; ATG, antithymocyte globulin; and CsA, cyclosporine A.

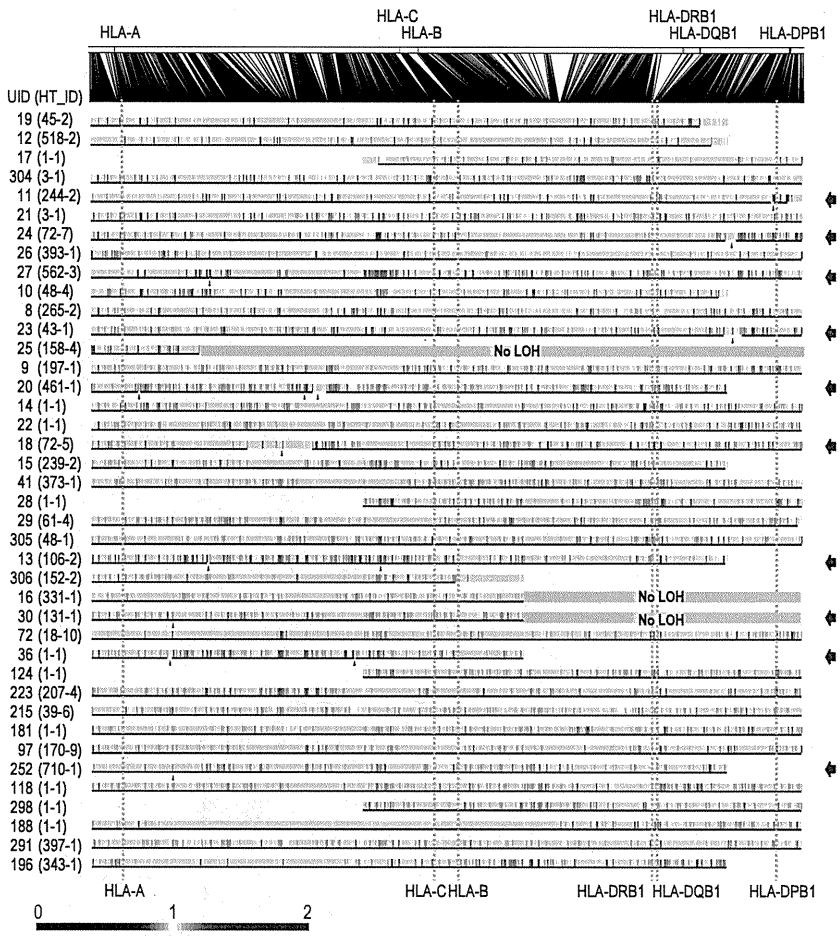

Figure 4. Imputation of missing HLA haplotypes. The observed allelic copy numbers at heterozygous SNP sites along each candidate SNP haplotype are color-coded as indicated at the bottom. Green bars showed the SNPs that are incompatible with the patient's genotype. Case IDs and haplotype ID (HT_ID) are indicated on the left. The locations of the 500K SNPs and HLA-A, C, B, DRB1, DQB1, and DPB1 are indicated in the figure. For each allele, genomic copy numbers were imputed using the circular binary segmentation algorithm. This divided each haplotype into one or more segments having discrete mean allelic copy numbers (blue arrows on the right). The positions of breakpoints are indicated by arrowheads. Finally, the mean allelic copy number of each segment was statistically compared with that of the corresponding segment on the other haplotype using the Wilcoxon signed rank test. Missing HLA haplotypes were determined based on the result of the statistic tests. Purple and blue lines indicated the retained and missing segments, respectively, whereas the allelic status was not determined statistically for those segments shown by green lines.

than these 4 alleles), where the odds ratios for the risk of the development of AA between each of these alleles and nonsignificant alleles were 1.87 (95% confidence interval [CI], 1.43-2.43) for A*02:01, 2.22 (95% CI, 1.70-2.90) for A*02:06, 1.37 (95% CI, 1.00-1.88) for A*31:01, and 1.95 (1.48-2.58) for B*40:02 (Table 4). The combined relative risk for all these alleles was 1.75 (1.42-2.17; $P = 1.3 \times 10^{-7}$).

Discussion

The origin of clonal hematopoiesis in AA is a focus of long-standing disputes, in which a profoundly reduced hematopoietic stem cell pool and/or escape from the autoimmune insults have been implicated in the evolution of the clonal hematopoiesis in AA.[5,22,23] Our findings on 6pLOH in AA provide an intriguing insight not only into the underlying mechanism of the clonal hematopoiesis in AA but also into the origin of the autoimmunity that is responsible for the pathogenesis of AA. A recent study from the United States also reported 3 cases with 6pLOH.[24] With a sensitive detection algorithm, the presence of the 6pLOH(+) components was demonstrated in as many as 13% of typical cases with AA, and the evidence from the subsequent studies strongly indicated that the HLA genes are the genetic targets of 6pLOH in AA patients. First, the HLA locus was commonly and critically involved in all 6pLOHs found in AA. Second, some AA patients carried multiple 6pLOH(+) subclones with different breakpoints, but in all cases, the 6pLOH involved the HLA locus and occurred in a manner that targeted the same parental HLA allele. Moreover, particular class I HLA alleles were over-represented among 6pLOH(+) cases and consistently found in the missing haplotypes. Finally, many of these HLA alleles were shown to be tightly

Table 4. Association of missing HLA alleles with AA in Japanese patients

Risk allele	AA (N = 407)	Other diseases (N = 6206)	Total (N = 6613)	P (χ^2 test)	Odds ratio (95% CI) (vs no risk alleles)
A*02:01	103	1173	1276	2.5×10^{-6}	1.87 (1.43–2.43)
A*02:06	100	957	1057	$< 1.0 \times 10^{-7}$	2.22 (1.70–2.90)
A*31:01	58	899	957	0.048	1.37 (1.00–1.88)
B*40:02	86	938	1024	1.8×10^{-6}	1.95 (1.48–2.58)
All risk alleles	268	3250	3518	1.3×10^{-7}	1.75 (1.42–2.17)
No risk alleles	139	2956	3095	—	—

— indicates not applicable.

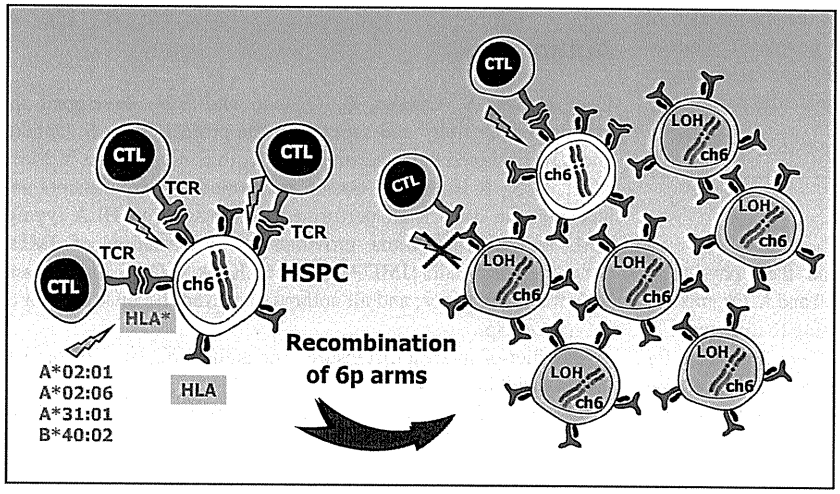

Figure 5. A proposed mechanism for escape hematopoiesis in 6pLOH(+) AA. In AA, the targets of CTLs are the HSPCs that present some auto-antigen through particular class I HLA molecules, including HLA-A*02:01, A*02:06, A*31:01, and B*40:02. In the presence of these autoimmune insults, the HSPCs that lose their expression of the antigen-presenting HLA molecule as a result of CNN-LOH in 6p would acquire a growth advantage over other HSPCs expressing the relevant HLA, leading to clonal outgrowth of the 6pLOH(+) progenies.

associated with the development of AA in Japanese patients in case-control studies using the large JMDP registry.

The conspicuous bias of the missing HLA alleles in 6pLOH to particular HLA types and the significant association of AA with those HLA types strongly suggest that the recurrent 6pLOH in AA is a phenomenon tightly related to the pathogenesis of AA rather than mere secondary event during the course of AA. Based on these observations, it is well reasoned that, in 6pLOH(+) AA cases, the autoimmunity to HSPCs is mediated by the CTLs that target the antigens presented via specific class I HLA molecules and that the 6pLOH(+) cells found in AA could be explained as escape hematopoiesis that survives the autoimmune insult by genetically deleting the relevant HLA species that are required for antigen presentation (Figure 5). These scenarios are further supported by the recent reports showing that the CNN-LOH in 6p provides a common mechanism of leukemic relapse after HLA haploidentical stem cell transplantations, in which leukemic cells that lost the mismatched HLA haplotype through CNN-LOH in 6p are thought to escape the immunologic surveillance of the engrafted donor T cells.[25,26] Importantly, it was experimentally demonstrated by immunologic assays that the 6pLOH(+) leukemic cells actually escaped GVL by CTLs, whereas 6pLOH(−) leukemic cells were effectively killed by the same CTLs. Although the immunologic targets of CTLs are different between relapse after haploidentical transplants (mismatched HLAs themselves) and AA (still unknown autoantigens presented on missing HLAs), the prominent similarities found in both cases further support that CNN-LOH in 6p confers an escape mechanism from autoreactive CTLs in AA.

In light of the above considerations, the chronologic behavior of the 6pLOH(+) components in PB is also interesting and worth discussing. Despite the assumption that 6pLOH is an effective escape mechanism from CTLs, the 6pLOH(+) stem cells were unable to repopulate the BM to cure AA, unless effective IST was applied (supplemental Figure 6). This is most probably explained by the presence of inflammatory cytokines, such as IFN-γ and TNF-α, which have also been shown to play an important role in the BM failure in AA and are thought to be responsible for the continued prevention of the 6pLOH(+) stem cells from fully expanding and reconstituting the BM (supplemental Figure 9A-B).[27,28]

When the autoimmune insults are removed after IST, no further injury of normal stem cells would occur. However, this does not necessarily mean the surviving normal stem cells can eventually outnumber the 6pLOH(+) stem cells over time. Note that, once the autoimmune insults disappear, nothing could biologically or immunologically discriminate a 6pLOH(+) stem cell from a 6pLOH(−) stem cell (supplemental Figure 9A). In particular, a 6pLOH(+) stem cell and a 6pLOH(−) stem cell will produce the same number of progeny on average and feed the same number of mature blood cells. As a consequence, once established, the predominance of 6pLOH(+) stem cells over 6pLOH(−) stem cells should be maintained, after the severely reduced hematopoietic stem cell pool has been re-expanded with removal of the inciting autoimmunity. It is also of note that the recovery of myeloid components after IST, which are affected more strongly by 6pLOH than lymphoid cells, contributes to an apparent increase in 6pLOH components in the SNP array analysis in PB (supplemental Figure 6A).

One of the most significant findings in the current study is the identification of the HLA alleles that are over-represented in the Japanese AA populations, including HLA-A*31:01, B*40:02, A*02:01, and A*02:06. All of these HLA alleles belong to class I MHCs and thus are thought to be involved in the antigen presentation to CTLs. This provides another prominent example, in which specific HLA types play a critical role in the development of a human disease, and the information about these particular HLA types provides a solid basis on which we can ultimately isolate the relevant antigens responsible for the development of AA. Of particular note, there was a previous report indicating that HLA-B*40:02 and A*02:06 were over-represented in PNH as well as AA, although the study size was much smaller than the current study.[29] Combined with our study, these findings support the hypothesis that AA and PNH are the different outcomes of the same immunologic insult[5,30] and may also provide the genetic basis of the high prevalence of AA and PNH in East Asia.[31,32]

In some AA cases, hematopoiesis could be maintained over years by the progenitors that escaped and survived the inciting autoimmune insult by deleting the target HLA through CNN-LOH in 6p. Given that the 6pLOH was detected in only 13% of our series, it is probable that other escape mechanisms may also operate to maintain hematopoiesis in AA. Indeed, clonality was clearly demonstrated in 20% of the 6pLOH(−) cases in the human androgen receptor assay study (supplemental Figure 8). In addition, our SNP array analysis also revealed a variety of clonal abnormalities in AA cases (Figure 1), although it is still open to question

whether these abnormalities actually represent the mechanism of escape hematopoiesis or were related to some neoplastic process. Further studies on the genetic basis of the escape mechanisms would contribute to our understanding of the molecular pathogenesis of AA.

Acknowledgments

The authors thank the patients and donors and their physicians, including K. Kawakami of Suzuka General Hospital and A. Okamoto of Nagoya Daini Red Cross Hospital, for contributing to this study.

This work was supported in part by the Core Research for Evolutional Science and Technology, the Japan Science and Technology Agency, the Ministry of Education, Culture, Sports, Science and Technology of Japan (Grant-in-Aids for Scientific Research), and the Ministry of Health, Labor and Welfare of Japan (Grant-in-Aids).

Authorship

Contribution: S. Ohtake, S. Ogawa, and S.N. developed the concept of the study and supervised the project; T.K., S. Ohtake, and S.N. designed the experiments; T.K., A.S.-O., Y. Sato, Y. Mori, M.K., M.S., K.H., and Y. Sasaki performed the experiments and analyzed the data; K.K. performed high-resolution HLA typing; S.M. and Y. Morishima provided the information of JMDP donor-recipient pairs (JMDP dataset); T.K., A.S.-O., S. Ogawa, and S.N. wrote the paper; and all authors approved the final version of the manuscript.

Conflict-of-interest disclosure: The authors declare no competing financial interests.

Correspondence: Shinji Nakao, Cellular Transplantation Biology, Kanazawa University Graduate School of Medical Science, 13-1 Takaramachi, Kanazawa, Ishikawa 920-8640 Japan; e-mail: snakao@med3.m.kanazawa-u.ac.jp.

References

1. Young NS, Calado RT, Scheinberg P. Current concepts in the pathophysiology and treatment of aplastic anemia. *Blood.* 2006;108(8):2509-2519.
2. Nakao S, Takami A, Takamatsu H, et al. Isolation of a T-cell clone showing HLA-DRB1*0405-restricted cytotoxicity for hematopoietic cells in a patient with aplastic anemia. *Blood.* 1997;89(10):3691-3699.
3. Chen J, Ellison FM, Eckhaus MA, et al. Minor antigen h60-mediated aplastic anemia is ameliorated by immunosuppression and the infusion of regulatory T cells. *J Immunol.* 2007;178(7):4159-4168.
4. Risitano AM, Maciejewski JP, Green S, Plasilova M, Zeng W, Young NS. In-vivo dominant immune responses in aplastic anaemia: molecular tracking of putatively pathogenetic T-cell clones by TCR beta-CDR3 sequencing. *Lancet.* 2004;364(9431):355-364.
5. Young NS. The problem of clonality in aplastic anemia: Dr Dameshek's riddle, restated. *Blood.* 1992;79(6):1385-1392.
6. Tiu R, Gondek L, O'Keefe C, Maciejewski JP. Clonality of the stem cell compartment during evolution of myelodysplastic syndromes and other bone marrow failure syndromes. *Leukemia.* 2007;21(8):1648-1657.
7. Lewis SM, Dacie JV. The aplastic anaemia-paroxysmal nocturnal haemoglobinuria syndrome. *Br J Haematol.* 1967;13(2):236-251.
8. Dameshek W. Riddle: what do aplastic anemia, paroxysmal nocturnal hemoglobinuria (PNH) and "hypoplastic" leukemia have in common? *Blood.* 1967;30(2):251-254.
9. Socie G, Rosenfeld S, Frickhofen N, Gluckman E, Tichelli A. Late clonal diseases of treated aplastic anemia. *Semin Hematol.* 2000;37(1):91-101.
10. Tichelli A, Gratwohl A, Wursch A, Nissen C, Speck B. Secondary leukemia after severe aplastic anemia. *Blut.* 1988;56(2):79-81.
11. de Planque MM, Kluin-Nelemans HC, van Krieken HJ, et al. Evolution of acquired severe aplastic anaemia to myelodysplasia and subsequent leukaemia in adults. *Br J Haematol.* 1988;70(1):55-62.
12. van Kamp H, Landegent JE, Jansen RP, Willemze R, Fibbe WE. Clonal hematopoiesis in patients with acquired aplastic anemia. *Blood.* 1991;78(12):3209-3214.
13. Kawase T, Morishima Y, Matsuo K, et al. High-risk HLA allele mismatch combinations responsible for severe acute graft-versus-host disease and implication for its molecular mechanism. *Blood.* 2007;110(7):2235-2241.
14. Nannya Y, Sanada M, Nakazaki K, et al. A robust algorithm for copy number detection using high-density oligonucleotide single nucleotide polymorphism genotyping arrays. *Cancer Res.* 2005;65(14):6071-6079.
15. Yamamoto G, Nannya Y, Kato M, et al. Highly sensitive method for genomewide detection of allelic composition in nonpaired, primary tumor specimens by use of affymetrix single-nucleotide-polymorphism genotyping microarrays. *Am J Hum Genet.* 2007;81(1):114-126.
16. Storey JD, Tibshirani R. Statistical significance for genomewide studies. *Proc Natl Acad Sci U S A.* 2003;100(16):9440-9445.
17. Ogawa S, Matsubara A, Onizuka M, et al. Exploration of the genetic basis of GVHD by genetic association studies. *Biol Blood Marrow Transplant.* 2009;15(1 suppl):39-41.
18. Morishima S, Ogawa S, Matsubara A, et al. Impact of highly conserved HLA haplotype on acute graft-versus-host disease. *Blood.* 2010;115(23):4664-4670.
19. Olshen AB, Venkatraman ES, Lucito R, Wigler M. Circular binary segmentation for the analysis of array-based DNA copy number data. *Biostatistics.* 2004;5(4):557-572.
20. Venkatraman ES, Olshen AB. A faster circular binary segmentation algorithm for the analysis of array CGH data. *Bioinformatics.* 2007;23(6):657-663.
21. Ishiyama K, Chuhjo T, Wang H, Yachie A, Omine M, Nakao S. Polyclonal hematopoiesis maintained in patients with bone marrow failure harboring a minor population of paroxysmal nocturnal hemoglobinuria-type cells. *Blood.* 2003;102(4):1211-1216.
22. Murakami Y, Kosaka H, Maeda Y, et al. Inefficient response of T lymphocytes to glycosylphosphatidylinositol anchor-negative cells: implications for paroxysmal nocturnal hemoglobinuria. *Blood.* 2002;100(12):4116-4122.
23. Bessler M, Mason PJ, Hillmen P, et al. Paroxysmal nocturnal haemoglobinuria (PNH) is caused by somatic mutations in the PIG-A gene. *EMBO J.* 1994;13(1):110-117.
24. Afable MG 2nd, Wlodarski M, Makishima H, et al. SNP array-based karyotyping: differences and similarities between aplastic anemia and hypocellular myelodysplastic syndromes. *Blood.* 2011;117(25):6876-6884.
25. Vago L, Perna SK, Zanussi M, et al. Loss of mismatched HLA in leukemia after stem-cell transplantation. *N Engl J Med.* 2009;361(5):478-488.
26. Villalobos IB, Takahashi Y, Akatsuka Y, et al. Relapse of leukemia with loss of mismatched HLA resulting from uniparental disomy after haploidentical hematopoietic stem cell transplantation. *Blood.* 2010;115(15):3158-3161.
27. Zoumbos NC, Gascon P, Djeu JY, Trost SR, Young NS. Circulating activated suppressor T lymphocytes in aplastic anemia. *N Engl J Med.* 1985;312(5):257-265.
28. Hinterberger W, Adolf G, Aichinger G, et al. Further evidence for lymphokine overproduction in severe aplastic anemia. *Blood.* 1988;72(1):266-272.
29. Shichishima T, Noji H, Ikeda K, Akutsu K, Maruyama Y. The frequency of HLA class I alleles in Japanese patients with bone marrow failure. *Haematologica.* 2006;91(6):856-857.
30. Karadimitris A, Manavalan JS, Thaler HT, et al. Abnormal T-cell repertoire is consistent with immune process underlying the pathogenesis of paroxysmal nocturnal hemoglobinuria. *Blood.* 2000;96(7):2613-2620.
31. Issaragrisil S, Kaufman DW, Anderson T, et al. The epidemiology of aplastic anemia in Thailand. *Blood.* 2006;107(4):1299-1307.
32. Montane E, Ibanez L, Vidal X, et al. Epidemiology of aplastic anemia: a prospective multicenter study. *Haematologica.* 2008;93(4):518-523.

Enucleation of human erythroblasts involves non-muscle myosin IIB

Kumi Ubukawa,[1] Yong-Mei Guo,[1] Masayuki Takahashi,[2] Makoto Hirokawa,[1] Yoshihiro Michishita,[1] Miho Nara,[1] Hiroyuki Tagawa,[1] Naoto Takahashi,[1] Atsushi Komatsuda,[1] Wataru Nunomura,[3-5] Yuichi Takakuwa,[3] and Kenichi Sawada[1]

[1]Department of Hematology, Nephrology, and Rheumatology, Akita University Graduate School of Medicine, Akita, Japan; [2]Division of Chemistry, Graduate School of Science, Hokkaido University, Hokkaido, Sapporo, Japan; [3]Department of Biochemistry, Tokyo Women's Medical University, Tokyo, Japan; and [4]Center for Geo-Environmental Science and [5]Department of Life Science, Graduate School of Engineering and Resource Science, Akita University, Akita, Japan

Mammalian erythroblasts undergo enucleation, a process thought to be similar to cytokinesis. Although an assemblage of actin, non-muscle myosin II, and several other proteins is crucial for proper cytokinesis, the role of non-muscle myosin II in enucleation remains unclear. In this study, we investigated the effect of various cell-division inhibitors on cytokinesis and enucleation. For this purpose, we used human colony-forming unit-erythroid (CFU-E) and mature erythroblasts generated from purified CD34$^+$ cells as target cells for cytokinesis and enucleation assay, respectively. Here we show that the inhibition of myosin by blebbistatin, an inhibitor of non-muscle myosin II ATPase, blocks both cell division and enucleation, which suggests that non-muscle myosin II plays an essential role not only in cytokinesis but also in enucleation. When the function of non-muscle myosin heavy chain (NMHC) IIA or IIB was inhibited by an exogenous expression of myosin rod fragment, myosin IIA or IIB, each rod fragment blocked the proliferation of CFU-E but only the rod fragment for IIB inhibited the enucleation of mature erythroblasts. These data indicate that NMHC IIB among the isoforms is involved in the enucleation of human erythroblasts. (*Blood.* 2012;119(4):1036-1044)

Introduction

During erythropoiesis, stem cells undergo lineage specific commitment and generate erythroid progenitor cells through cellular division events including nuclear (mitosis) and cytoplasmic (cytokinesis) division. These progenitor cells consist of immature and mature erythroid progenitors, the burst-forming unit-erythroid (BFU-E) and the colony-forming unit-erythroid (CFU-E), respectively. The BFU-E can be considered as a progenitor of the CFU-E. Indeed, after 6 to 7 days in culture, cells generated from human BFU-E have all the functional characteristics of CFU-E[1]. After an additional 6 to 7 days in culture, human CFU-E proliferate and differentiate into mature erythroblasts.[1] Terminally differentiated erythroblasts in mammals expel their nuclei via a process termed enucleation, becoming reticulocytes and subsequently mature erythrocytes. The nucleus separates from the remainder of the cell and is phagocytosed by reticular cells such as macrophages (for a review, see Chasis et al[2]).

Enucleation of erythroblasts is thought to occur through a process similar to cytokinesis. Several general principles apply to cytokinesis. Firstly, the microtubule cytoskeleton plays an important role in both the choice and positioning of the division site. Once this site is chosen, the local assembly of the actomyosin contractile ring remodels the plasma membrane. Finally, membrane trafficking to, and membrane fusion at the division site result in the physical separation of the daughter cells, a process termed abscission (for reviews, see Barr et al[3] and Glotzer et al[4]). Although modulation of the actomyosin cytoskeleton is crucial for proper cytokinesis, there is a paucity of information regarding how non-muscle myosin II contributes to enucleation.

Several investigations have studied the molecular mechanisms underlying the enucleation of mammalian erythroblasts. Koury et al used murine splenic erythroblasts infected with the anemia-inducing strain of Friend-virus (FVA cells), and demonstrated that filamentous actin (F-actin) accumulated in the contractile ring.[5] They also showed that the treatment of FVA cells with cytochalasin D blocked nuclear extrusion, while the addition of colchicine, vinblastine or taxol did not affect enucleation.[5] Based on these findings, they concluded that F-actin plays an important role in enucleation, while microtubules do not. It has also been shown that Rac 1 GTPases and their downstream effector mDia2 play important roles in the cytoskeletal reorganization that leads to the extrusion of the pycnotic nucleus from late-stage erythroblasts.[6] Recently, important roles for Myc,[7] Claudin 13[8] (a member of the Claudin family of tight junction proteins), histone deacetylase 2,[9] and membrane trafficking[10] have been reported in the regulation of terminal maturation in mammalian erythroid cells.

Non-muscle myosin II is a major cytoskeletal protein that interacts with actin to contribute to cellular processes such as cell migration,[11] cell adhesion,[12] and cytokinesis.[13] In mammals there are 3 non-muscle myosin II isoforms, each composed of one pair of heavy chains and 2 pairs of light chains. Three separate genes (*Myh 9, Myh10, and Myh 14*) encode the non-muscle myosin heavy chains (NMHCs; NMHC IIA, IIB, and IIC) in chromosomes 22q11.2, 17p13, and 19q13, respectively.[14-16] These isoforms share considerable homology and some overlapping functions, yet they exhibit differences in enzymatic properties, subcellular localization, molecular interaction and tissue distribution (for a review, see Even-Ram et al[17]). The mechanistic knowledge about non-muscle myosin II isoforms in enucleation may help us to explore the unknown NMHC abnormalities in hematologic disorders. Indeed, deficiency of non-muscle myosin II isoform can cause human disease. The 4 main autosomal dominant disorders are related to

Submitted June 17, 2011; accepted October 20, 2011. Prepublished online as *Blood* First Edition paper, November 2, 2011; DOI 10.1182/blood-2011-06-361907.

An Inside *Blood* analysis of this article appears at the front of this issue.

The online version of this article contains a data supplement.

The publication costs of this article were defrayed in part by page charge payment. Therefore, and solely to indicate this fact, this article is hereby marked "advertisement" in accordance with 18 USC section 1734.

mutations in *Myh 9*, the gene for the NMHC IIA: May-Hegglin, Fechtner, Sebastian and Epstein (for a review, see Kunishima et al[18]). The common feature in all 4 syndromes is macrothrombocytopenia, and granulocyte inclusion bodies characterize the first 3 syndromes. Some patients later show onset of deafness, cataracts, and glomerulonephritis.[18]

In this study, we investigated the role of myosin in human erythroblast enucleation in association with other cytoskeletal molecules. The efficacy of inhibitors for cell division often varies depending on the species of the cell observed and their redundancy in the cells themselves.[19] Therefore, efficient inhibitors of cell division in human primary erythroid cells were selected using human CFU-E generated from purified $CD34^+$ cells to clarify the possible efficacy of these inhibitors on the enucleation of erythroblasts. Here we show that the inhibition of non-muscle myosin II ATPase by blebbistatin completely blocks enucleation of human erythroblasts. When the function of NMHC IIA or IIB was inhibited by an exogenous expression of myosin rod fragment, both rod fragments blocked the proliferation of CFU-E and the rod fragment for IIB inhibited the enucleation of mature erythroblasts. These data indicate that the enucleation of human erythroblasts involves non-muscle myosin IIB.

Methods

Reagents and antibodies

BSA, IMDM and propidium iodide (PI) were purchased from Sigma-Aldrich. FCS, penicillin and streptomycin were obtained from Flow Laboratories Inc. Insulin (porcine sodium, activity 28.9 U/mg) was obtained from Wako Pure Chemical Industries. IL-3 and SCF were kind gifts from Kirin Brewery Co Ltd, and erythropoietin (EPO) and G-CSF were from Chugai Pharmaceutical Co. Vitamin B_{12} was purchased from Eisai Co Ltd and folic acid was from Takeda Pharmaceutical Co Ltd. Triton X-100 was obtained from Wako Pure Chemical Industries. Diaminobenzidine-substrate chromogen and fuchsin-substrate chromogen systems were from Dako. RNase (Type III-A) was from Sigma-Aldrich. MACS MicroBeads for Indirect Magnetic Labeling was from Miltenyi Biotec. FITC-labeled and phycoerythrin (PE)–labeled antibodies for glycophorin A (GPA; JC159) were from Dako. Alexa Fluor 488– or Alexa Fluor 546–conjugated goat IgG directed against rabbit and mouse IgG were from Molecular Probes. Fc-blocking antibody (anti-CD16/32, clone: 93) was from eBioscience. Normal mouse and goat sera and rabbit immunoglobulins were from CellSignaling Technology. Alexa Fluor 488 phalloidin was from Invitrogen. Rabbit polyclonal antibody to non-muscle myosin IIA was from Sigma-Aldrich or Covance. Rabbit polyclonal antibody to non-muscle myosin IIB was from Abcam or Cell Signaling Technology. Mouse monoclonal antibody to tublin-α was from Neo Markers. Goat anti–mouse IgG-HRP was from Santa Cruz Biotechnology Inc. Anti–rabbit IgG, HRP-linked antibody and myosin light chain 2 antibody sampler kit were from Cell Signaling Technology. Amersham ECL Plus Western Blotting detection reagents were from GE Healthcare. Novex Sharp protein standard and NuPAGE Novex Bis-Tris mini gels were from Invitrogen.

Cell division inhibitors

Blebbistatin, a small molecule inhibitor that shows a high affinity and selectivity toward non-muscle myosin II ATPase,[20] and NSC23766, a specific inhibitor of Rac1 GTPases[21] that is known to inhibit enucleation,[6] were purchased from Calbiochem. Cytochalasin D, an inhibitor of actin polymerization that is known to inhibit enucleation,[5] and colchicine, an inhibitor of microtubules that are known to not be directly involved in enucleation[5] (for a review, see Wilson et al[22]), were purchased from Sigma-Aldrich. Y27632, a well-established inhibitor of ROCK that is a regulator of myosin phosphorylation,[23,24] was purchased from Enzo Life Sciences, Inc. Monastrol, an inhibitor of kinesin Eg5 which is a microtubule-based motor that plays a critical role in mitosis as it mediates centrosome separation and bipolar spindle assembly and maintenance,[25] was from Merck.

Cell preparations

G-CSF mobilized human peripheral blood $CD34^+$ cells were purified from healthy volunteers as described previously,[26] and stored in liquid nitrogen until required. Informed consent was obtained from each subject before their entry into this study, and the study was pre-approved by the Akita University Graduate School of Medicine Committee for the Protection of Human Subjects.

For the generation of erythroid progenitor cells, $CD34^+$ cells were thawed and prepared for culture as previously described.[27] Cells were cultured in IMDM erythroid medium containing 20% FBS, 10% heat-inactivated pooled human AB serum, 1% BSA, 10 μg/mL insulin, 0.5 μg/mL vitamin B_{12}, 15 μg/mL folic acid, 50nM β-mercaptoethanol (β-ME), 50 U/mL penicillin and 50 μg/mL streptomycin in the presence of 50 ng/mL IL-3, 50 ng/mL SCF and 2 IU/mL EPO. Cells were maintained at 37°C in a 5% CO_2 incubator as described previously.[27] After 7 days in culture, cells (day 7 cells, D7) were harvested and washed 3 times with IMDM containing 0.1% BSA and stored at 4°C until required. The maturation levels of the day 7 cells were found to be similar to that of the colony-forming unit-erythroid (CFU-E), a finding that has been reported elsewhere.[27,28] As a result, day 7 cells are described as CFU-E throughout this report.

Aliquots of CFU-E were also cultured in the erythroid medium with EPO alone, but without β-ME, SCF and IL-3, and then cultured for additional days to induce differentiation with or without various inhibitors of cell division. The volume of inhibitors, H_2O, PBS and DMSO vehicle solutions was fixed to 5% of the erythroid medium. The final concentration of DMSO in the erythroid medium was fixed to 0.2% (vol/vol) as DMSO over this concentration is known to be toxic for human erythroid progenitors. The cells were harvested at various time points, washed 3 times with IMDM containing 0.1% BSA, resuspended in IMDM containing 0.1% BSA and stored at 4°C until required.

For the evaluation of the enucleation ratio, the cells were spun onto slides using a Cytospin 3 (Shandon Lipshaw Inc) and stained with May-Grünwald-Giemsa or o-dianisidine (for hemoglobin staining) and hematoxylin. Enucleation was defined as the expulsion of the nucleus to the outside of the reticulocyte. Reticulocytes that are touching expulsed nuclei or that have thin, connecting strand of cellular material between the reticulocyte and the nucleus were also considered the earliest cell that has enucleated (supplemental Figure 1, available on the *Blood* Web site; see the Supplemental Materials link at the top of the online article). The enucleation ratio of these cytospun cells was similar to that of cells prepared without mechanical force.[1] The enucleation ratio was calculated as [*Enucleation ratio* = erythrocytes/(erythrocytes+erythroblasts)] × 100% and by counting 300 cells including erythrocytes and erythroblasts on each slide. Triplicate cultures were used at each time point. The yield and viability were measured by dye exclusion using 0.2% trypan blue dye and a hemocytometer.

Cell cycle distribution

Cells were harvested, washed with cold PBS and fixed in 70% ethanol. The cells were then stored at −20°C until analysis. The fixed cells were centrifuged at 200*g*, washed with cold PBS twice, and RNase A was added at a final concentration of 0.5 mg/mL. The cells were then incubated for 10 minutes at 37°C. Next, 25 μg/mL PI was added and the cells were incubated for 30 minutes at room temperature in the dark. The cells were analyzed using a FACS Calibur instrument (BD Biosciences) equipped with CellQuest 3.3 software as reported previously.[29] Multicycle Version 4.0.0.4 cell cycle analysis software (Beckman Coulter) was used to determine the percentages of cells in the different cell cycle phases.